European Journal of Medicinal Chemistry 47 (2012) 239–254

Contents lists available at SciVerse ScienceDirect

European Journal of Medicinal Chemistry

journal homepage: http://www.elsevier.com/locate/ejmech

Original article

Identification of new aminoacid amides containing the imidazo[2,1-*b*]benzothiazol-2-ylphenyl moiety as inhibitors of tumorigenesis by oncogenic Met signaling

Alessandro Furlan [a,1], Francesco Colombo [b,1], Andrea Kover [c,1], Nathalie Issaly [a,1], Cristina Tintori [d], Lucilla Angeli [d], Vincent Leroux [e,f], Sébastien Letard [g], Mercedes Amat [c], Yasmine Asses [e], Bernard Maigret [e], Patrice Dubreuil [g], Maurizio Botta [d], Rosanna Dono [a,*****], Joan Bosch [c,****], Oreste Piccolo [h,***], Daniele Passarella [b,**], Flavio Maina [a,*]

[a] *Aix-Marseille Univ, IBDML, CNRS UMR 6216, Parc Scientifique de Luminy, Case 907, 13288 Marseille, France*
[b] *Dipartimento di Chimica Organica e Industriale, Università degli Studi di Milano, Via Venezian 21, 20133 Milano, Italy*
[c] *Laboratory of Organic Chemistry, Faculty of Pharmacy and Institute of Biomedicine (IBUB), University of Barcelona, 08028 Barcelona, Spain*
[d] *Dipartimento Farmaco Chimico Tecnologico, Università degli Studi di Siena, Via Alcide de Gasperi 2, I-53100 Siena, Italy*
[e] *Nancy Université, LORIA-UMR 7503, Equipe projet Orpailleur, Campus scientifique, BP 239, 54506 Vandœuvre-lès-Nancy Cedex, France*
[f] *University of Oslo, Chemistry Department, P.O. Box 1033 Blindern, 0315 Oslo, Norway*
[g] *Centre de Recherche en Cancérologie de Marseille – U891 INSERM, Institut Paoli-Calmettes, Université de la Méditerranée 27, boulevard Lei Roure BP 30059, 13273 Marseille Cedex 09, France*
[h] *Studio di consulenza scientifica, Via Bornò 5, 23896 Sirtori (LC), Italy*

ARTICLE INFO

Article history:
Received 9 June 2011
Received in revised form
30 September 2011
Accepted 27 October 2011
Available online 4 November 2011

Keywords:
Met RTK
Met signaling inhibitor
Inhibitor binding modes
Aminoacid-amide derivatives
Anti-tumor agents
Imidazo[2,1-*b*]benzothiazol-2-ylphenyl moiety

ABSTRACT

The Met receptor tyrosine kinase is a promising target in anticancer therapies for its role during tumor evolution and resistance to treatment. It is characterized by an unusual structural plasticity as its active site accepts different inhibitor binding modes. Such feature can be exploited to identify distinct agents targeting tumor dependence and/or resistance by oncogenic Met. Here we report the identification of bioactive agents, featuring a new 4-(imidazo[2,1-*b*]benzothiazol-2-yl)phenyl moiety, targeting cancer cells dependent on oncogenic Met. One of these compounds (**7c; Trifloreas**) impairs survival, anchorage-independent growth, and in vivo tumorigenesis, without showing side effects. Our medicinal chemistry strategy was based on an in-house Met-focused library of aminoacid-amide derivatives enriched through structure-based computer modeling, taking into account the Met multiple-binding-mode feature. Altogether, our findings show how a rational structure-based drug design approach coupled to cell-based drug evaluation strategies can be applied in medicinal chemistry to identify new agents targeting a given oncogenic-dependency setting.

1. Introduction

Receptor tyrosine kinase (RTK) signaling is one core pathway altered frequently in cancer. Therapeutic approaches based on compounds targeting selectively oncogenic RTKs, to which cells are dependent, are constantly developed [1–3]. Among those investigated anticancer drug targets, the Met RTK has drawn significant attention for the ability of its oncogenic forms to confer growth advantage, protection from apoptosis, invasive properties, and resistance to chemotherapies [4–6]. Met is activated upon binding of its natural ligand hepatocyte growth factor, also known as scatter factor (HGF/SF). Following its activation, the Met RTK triggers a number of signaling pathways that regulate specific biological

Abbreviations: RTK, Receptor tyrosine kinase; HGF, Hepatocyte growth factor; SF, Scatter factor; i.p., intraperitoneal; ATP, Adenosine triphosphate; IL-3, Interleukin-3; TPR, Translocated promoter region; MS, Mass spectrometry; DCC, Dicyclohexylcarbodiimide; DCI, Diisopropylcarbodiimide; HATU, 2-(7-azabenzotriazol-1-yl)-1,1,3,3-tetramethyluronium hexafluorophosphate; HOBt, 1-hydroxybenzotriazole; DIPEA, Diisopropylethylamine; DMAP, 4-N,N-dimethylaminopyridine; BOPCl, Bis(2-oxo-3-oxazolidinyl)phosphinic chloride; TFA, Trifluoroacetic acid; DMSO, Dimethyl sulfoxide; RMSD, Root mean square deviation.

* Corresponding author. Tel.: +33 4 91 26 97 69.
** Corresponding author. Tel.: +39 02 50 31 40 81.
*** Corresponding author. Tel.: +39 39 39 47 98 70.
**** Corresponding author. Tel.: +34 93 402 45 38.
***** Corresponding author. Tel.: +33 4 91 26 92 66.
E-mail addresses: rosanna.dono@ibdml.univmed.fr (R. Dono), joanbosch@ub.edu (J. Bosch), orestepiccolo@tin.it (O. Piccolo), Daniele.passarella@unimi.it (D. Passarella), flavio.maina@ibdml.univmed.fr (F. Maina).
URL: http://www.maina-ibdml.eu
[1] These authors contributed equally to this work.

0223-5234/$ – see front matter © 2011 Elsevier Masson SAS. All rights reserved.
doi:10.1016/j.ejmech.2011.10.051

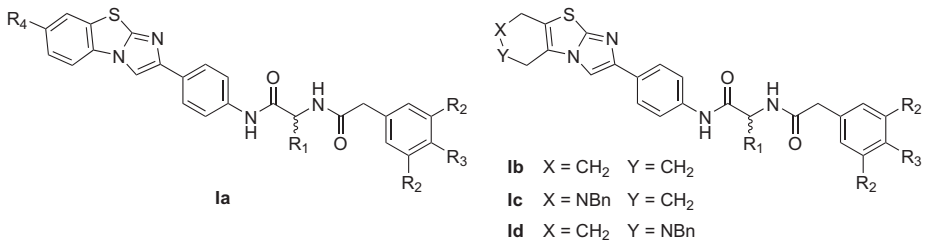

Fig. 1. Compounds of general formula **Ia**–**d**.

events during development [7–12,50] and regenerative processes [13,14], but also tumorigenesis [4,6,15]. Moreover, during tumor evolution oncogenic Met confers oncogene addiction, drug and/or radiotherapy resistance [16–20]. Therefore, agents able to antagonize oncogenic Met are expected to have a strong impact in molecularly targeted therapies for different types of human cancers. The great importance given to anti-Met agents for anticancer treatment as well as for fighting against resistance mechanisms caused by activated Met is mirrored by several research attempts to discover small-molecule inhibitors (see Supporting Information) [21,22]. However, the relatively high number of Met inhibitors already available does not deter academic labs and biopharma companies from investing persistent efforts aimed at uncovering novel compounds. This is shown also by the constant stream of released crystallographic complexes on the Protein Data Bank (PDB) database [23].

The Imatinib successful story has demonstrated that kinase inhibitors can effectively target specific inactive kinase conformations, allowing for the design of selective drugs [24,25]. This fostered tremendous research efforts in the industry for designing a new generation of anticancer drugs [26]. It is now acknowledged that upon the binding of ATP-competitive inhibitors, RTKs may adapt three distinct binding modes. However, RTKs currently known as able to accommodate all three kinds of inhibitor binding (to the RTK active state, DFG-out inactive state, and C-helix-out inactive state) are rare [27]. By applying molecular modeling and molecular mechanics to analyze the distribution of ligand interactions on Met residues as shown on available X-ray complexes, we previously demonstrated that Met is among the few RTKs accepting the three possible binding modes [28]. It has already been reported that the striking Met RTK plasticity, at the time with two known binding modes [29], is a clear opportunity for designing new Met-targeting compounds. We present the first study, to our knowledge, of a medicinal chemistry attempt aided by rational structure-oriented modeling, taking explicitly into account the triple-binding-mode feature of Met.

We report here in silico modeling studies, the synthesis, and the biological characterization of a new class of aminoacid amide derivatives, containing a 4-(imidazo[2,1-*b*]benzothiazol-2-yl) phenyl moiety (**Ia**, Fig. 1). Compounds were first biologically evaluated for their ability to impair Met-triggered cell scattering in vitro. Detailed in vitro biological characterization showed that distinct members of this new class of compounds impair survival and anchorage-independent growth of cancer cells addicted to oncogenic Met. A cell-based screen revealed selectivity toward the Met family members. These agents did not cause any major toxic effect neither on primary neuron nor on hepatocyte cultures. Finally, in vivo studies proved anti-tumor effects of the most active compound toward Met-addicted cancer cells, without causing side effects. Thus, our studies show how multidisciplinary strategies including in silico structure-based drug design and a cell-based focused drug screen can lead to the generation of agents that contrast tumorigenesis triggered by oncogenic signals like those emanating from the Met RTK.

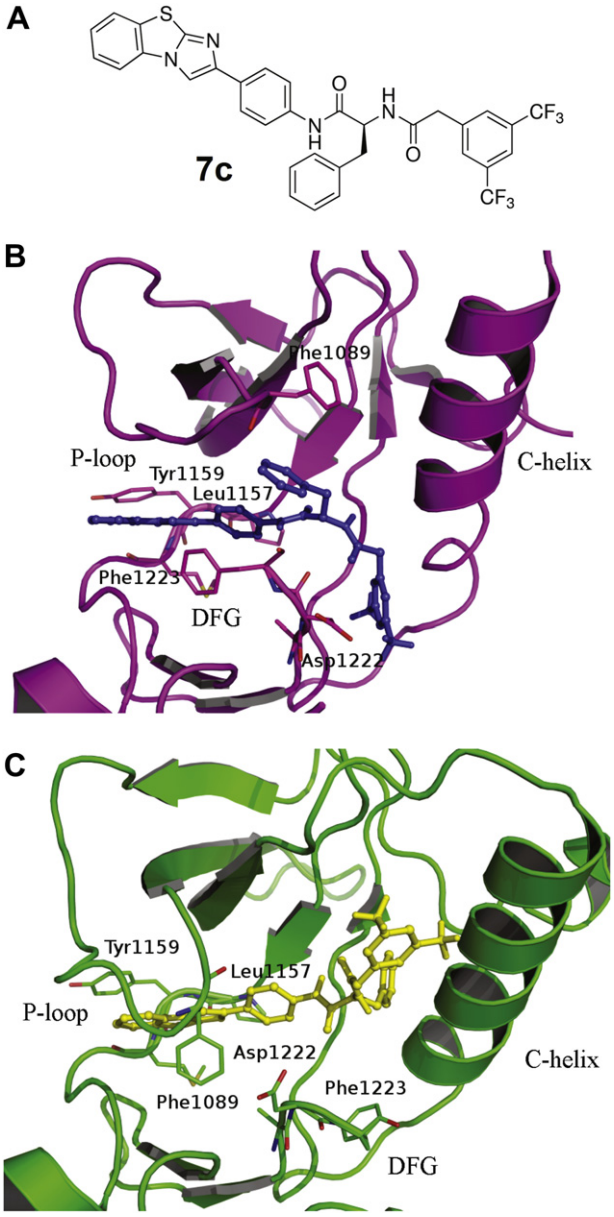

Fig. 2. Computer modeling shows that compound **7c** interacts with the Met ATP binding pocket. (A) 2D structure of compound **7c** (CF052). (B) Binding mode of compound **7c** (blue) within the 3CTJ structure (purple). (C) Binding mode of compound **7c** (yellow) within the 3EFK X-ray structure (green). (For interpretation of the references to color in this figure legend, the reader is referred to the web version of this article.)

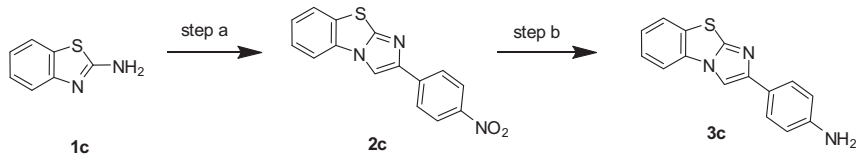

Scheme 1. Synthesis of compound **3c**. Step a: 2-bromo-4′-nitroacetophenone, EtOH or i-PrOH, reflux, 90 min. Step b: Fe in HCl 12N, H_2O, EtOH, reflux, 90 min or $SnCl_2$, HCl 12N, MeOH, reflux, 90 min. A similar strategy was adopted for the synthesis of other compounds (**3a**, **3b**, **3d**, and **3e**).

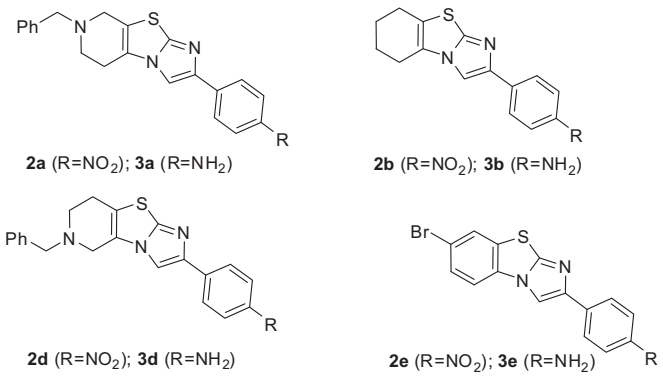

Scheme 2. Intermediates **2** and **3** prepared.

2. Results

2.1. Computer-aided rational design

2.1.1. Rational design of a Met-focused virtual library and docking calculations to select potential inhibitors for experimental investigation

A starting series of compounds was modeled from in-house organic chemistry knowledge and analysis of known anticancer compounds reported in the IMS Pioneer (http://www.imshealth.com) and Becker's Pharma Market (http://www.beckerpharmaceuticals.com) databases. The small molecules were first subjected to docking calculations, using as target models the experimentally-derived Met RTK conformation available in the PDB: 1R0P [30]. Results were analyzed by both molecular modelers and organic chemists, leading to an incremental virtual library design process that was followed as long as clear improvements of average docking performance were achieved. Subsequent docking studies were performed (see Experimental Protocol section) and a subset of best molecules was identified on the basis of scoring function values. Analysis of this subset suggested optimal functional groups and/or regions where improvements could possibly be further made. Based on this information, devised probable chemically-feasible optimizations were further made, resulting in a new family of candidate agents. It should be noted that docking program scoring functions were applied to identify probable structural optimizations from a set of compounds with similar chemical features rather than for hit prediction, as we do not consider it accurate enough for such a purpose. Through a repeated process merging organic chemistry and molecular model knowledge, a total of 2275 structures (2559, counting stereoisomers) were analyzed through 7 generation/optimization steps. The aforementioned process started with 2146 compounds, with a subsequent selection process leading progressively to 22, 15, 35, 28, and 18 molecules, resulting to a final group of 11 compounds (Supplementary Table 1).

Docking studies were then performed using two other experimentally-derived Met conformations from the PDB: 2RFN and 2RFS [31]. In 2RFS, Met is bound to the SU11274 kinase inhibitor, with a binding mode similar to the 1R0P's K-252a staurosporine analog (kinase active state). The 2RFN conformation corresponds to the Met-compound (AM7) binding in an inactive C-helix-out type state [28,29]. These analyses showed that we indeed selected optimal compounds for targeting the 1R0P conformation, as both the average and best scoring functional values were improved through the 7 generations (Supplementary Table 1). Surprisingly, for the 57 compounds corresponding to generation 5–7, we found that their scores were optimal for both 1R0P and 2RFN conformations, and, to a lesser extent, for 2RFS. These

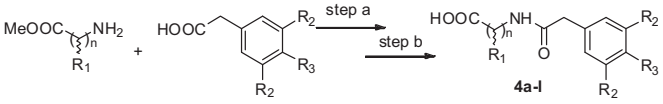

Compound	n	R_1	R_2	R_3
4a	1	(*S*)-Bn	CH_3	H
4b	1	(*R*)-Bn	CH_3	H
4c	1	(*S*)-Bn	CF_3	H
4d	1	(*R*)-Bn	CF_3	H
4e	1	(*S*)-Bn	F	H
4f	1	H	CH_3	H
4g	1	(*S*)-*p*OH-$C_6H_4CH_2$	CH_3	H
4h	2	H	F	H
4i	1	(*R*)-CH_2S-Tr*	F	H
4j	1	(*S*)-Me	F	H
4k	1	(*R*)-Me	F	H
4l	1	(*S*)-Bn	H	CH_3

Scheme 3. Synthesis of compounds **4a**–**l**. Step a: DCC or DCI, THF, room temperature (rt), 48 h. Step b: NaOH 1 M, MeOH, rt, 1 h *Tr = trityl (triphenylmethyl group).

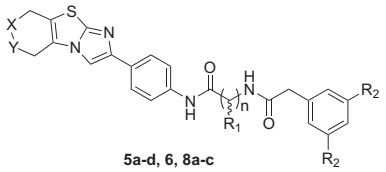

Compound	n	X	Y	R_1	R_2
5a	1	NCH_2Ph	CH_2	(*S*)-Bn	Me
5b	1	NCH_2Ph	CH_2	(*R*)-Bn	Me
5c	2	NCH_2Ph	CH_2	H	F
5d	1	NCH_2Ph	CH_2	(*R*)-CH_2SH^*	F
6	1	CH_2	CH_2	(*S*)-Bn	Me
8a	2	CH_2	NCH_2Ph	H	F
8b	1	CH_2	NCH_2Ph	(*S*)-Me	F
8c	1	CH_2	NCH_2Ph	(*R*)-Me	F

Scheme 4. Compounds **5**, **6**, and **8** prepared. *The trityl group was removed, after condensation, as reported in the experimental section.

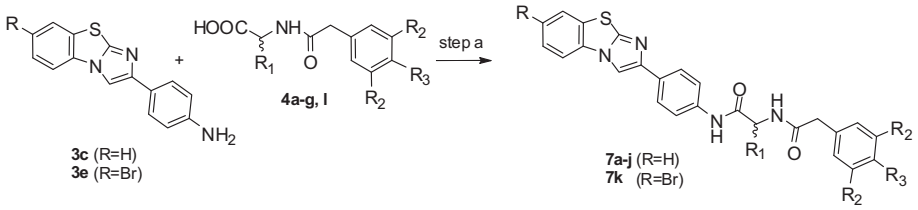

Compound	Code	R	R_1	R_2	R_3
7a	CF022	H	(*S*)-Bn	CH_3	H
7b	CF056	H	(*R*)-Bn	CH_3	H
7c	CF052 (Triflorcas)	H	(*S*)-Bn	CF_3	H
7d	CF081	H	(*R*)-Bn	CF_3	H
7e	CF082	H	(*S*)-Bn	F	H
7f	CF083	H	H	CH_3	H
7g	CF023	H	(*S*)-*p*OH-$C_6H_4CH_2$	CH_3	H
7h	CF201	H	(*S*)-Bn	H	CH_3
7i	CF207	H	(*S*)-*p*CH_3-$C_6H_4CH_2$	CH_3	H
7j	CF209	H	(*S*)-*p*CH_3-$C_6H_4CH_2$	CF_3	H
7k	CF203	Br	(*S*)-Bn	CF_3	H

Scheme 5. Synthesis of compounds **7a**–**h**,**k**. Step a: HATU, DIPEA, THF, rt, 16h or BOPCl, HOBt, DIPEA, CH_2Cl_2, rt, 48 h. Compounds **7i** and **7j** were prepared with a different procedure as reported in the experimental section.

outcomes may originate from the virtual screening protocol and the design choices, and suggest that compounds highlighted from our virtual library could be either inhibitor targeting an inactive Met RTK conformation, or dual-specificity inhibitors that could be further optimized. Summarizing all gathered data, two distinct classes of compounds, characterized by a kinase inhibitor profile, were highlighted. One of these two is defined by the imidazo[2,1-*b*] benzothiazol-2-ylphenyl moiety (**Ia**, Fig. 1), with some chemical features shared with another series of Met inhibitors that we were investigating (**Ib**–**d**, Fig. 1) [32]. **Ia**-based compounds were selected for chemical synthesis and biological evaluation, resulting in the present publication.

2.1.2. Molecular modeling of ***Ia*** compounds in complex with the Met RTK

In parallel to chemistry and biology experimental efforts dedicated to the **Ia** class (described in the next sections), computer models of the corresponding protein–ligand complexes were generated. Additional Met crystallographic complexes had been released in the PDB, allowing us to derive a precise molecular mechanics-based model for characterizing Met RTK interactions with inhibitors. It appeared that Met inhibitors could be clustered into three distinct families, corresponding to the active state, the DFG-out inactive state, and the C-helix-out inactive state [28]. Being capable of accepting these three ligand binding modes is an uncommon feature for kinases [27]. In order to optimally exploit this Met RTK bound conformational space, the **Ia** compounds were docked against each of those three possible states.

2.1.2.1. Docking on the active state conformation. Docking **Ia**-derived compounds on the conformation from the 2RFS complex [31] representative of the Met active state, resulted in significantly lower binding scores than with the two other inactive state conformations described below. This is not a surprising result, considering that the compounds we have designed possess structural properties typical of inactive-state-binding kinase inhibitors. Indeed, only Met inactivation may provide additional hydrophobic area (either by displacement of the A-loop or the C-helix) required to accommodate small molecules possessing an extended scaffold, such as **Ia**–**d**.

2.1.2.2. Docking on the DFG-out conformation. The 3CTJ X-ray complex [33] was selected as representative of the DFG-out inactive state (Fig. 2 is referred to **7c**). Fig. 2B shows compound **7c** (Triflorcas) bound to this model. The docking calculations showed a common binding mode for the left part of all inhibitors. The benzothiazole (A-ring) is bound to the hinge region and partially superimposed to the pyrrolopyridine found in the crystallographic complex. The central aromatic ring (B-ring) π-stacks with Phe1223 (DFG motif) and is flanked on the opposite face by hinge residue Leu1157. The –NH–CO–CH–NH chain is involved in H-bonds with Asp1222, Glu1127, and Nε of Lys1110. Interactions with these residues are consistently found among ligands bound to Met inactive states [28]. The **7c** bimethylfluorobenzyl fragment occupies the DFG pocket. Other ligands reported in this paper, upon docking to this conformation, share the same general orientation, with either their C- or D-ring occupying the DFG pocket.

2.1.2.3. Docking on the C-helix-out conformation. The 3EFK X-ray complex [34] was selected as representative of the Met C-helix-out inactive state. Fig. 2C shows the result with **7c**. Similarly to DFG-out docking results, the A-ring is found in the hinge region. The B-ring makes lipophilic interactions with the side chains of Leu1157 and Phe1089 (stacking) rather than with Phe1223 of the DFG triad. As a result, the C- and D-rings are oriented toward the C-helix and away from the A-loop. The **7c** C-ring binds to a small hydrophobic pocket formed around Ile1145 by C-helix displacement. At this stage, docking results suggest that **7c** and analogs may equally bind to either a DFG-out or C-helix-out inactive state Met conformation.

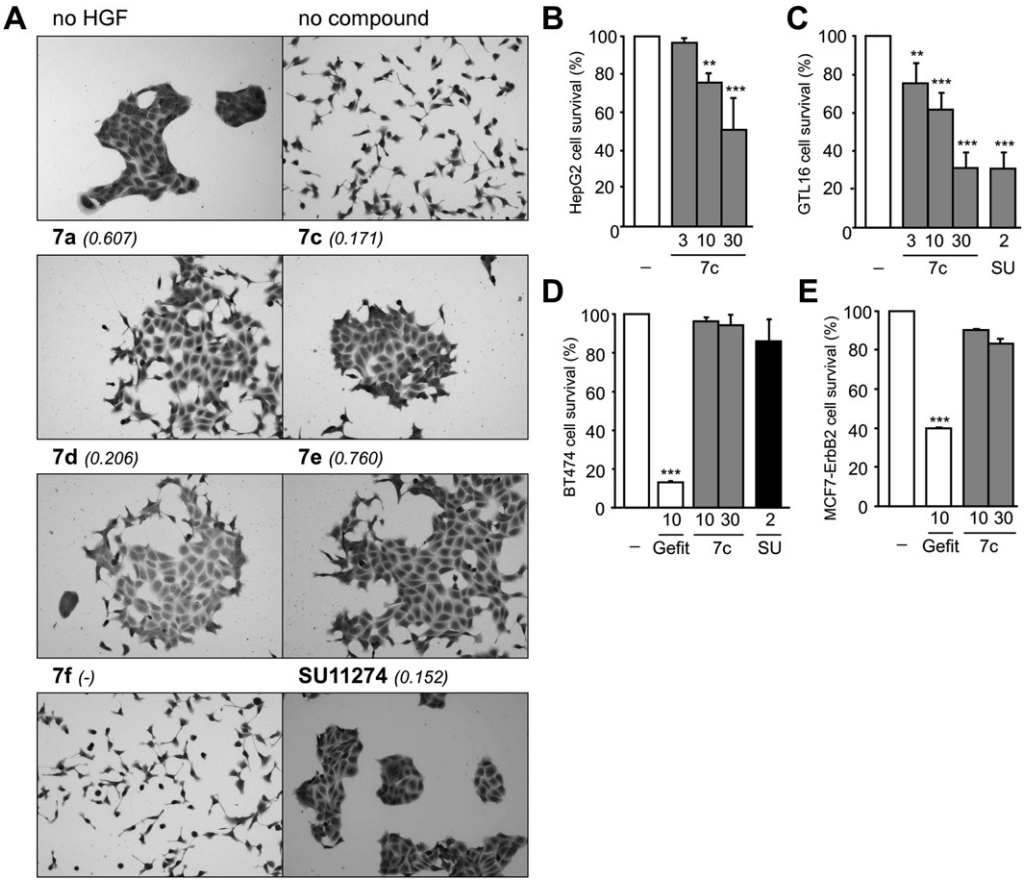

Fig. 3. Imidazo[2,1-*b*]benzothiazol-2-ylphenyl compounds block Met-triggered cell scattering and cell survival. (A) HGF-induced scattering of MDCK cells is blocked by **7a**, **7c**, **7d**, **7e**, and not by **7f**. SU11274 was used as positive control. The IC_{50} is indicated in μM. (B and C) Survival of HepG2 (B) and GTL-16 (C) cells was reduced by **7c**, in a dose dependent manner (μM). SU11274 (SU) was used at 2 μM (D and E) Survival of BT474 (D) and MCF7-ErbB2 (E) cells, which are addicted to the ErbB oncogenes, was impaired by the ErbB inhibitor Gefitinib (Gefit), but not by **7c** or by SU11274 (μM). For survival assays ($n = 3$), cells were serum-starved for 24 h and then incubated with **7c**, SU11274, or Gefitinib for 48 h. Values are expressed as means ± s.e.m. $^{**}P < 0.01$; $^{***}P < 0.001$; Student-*t* test.

2.2. Chemistry

To synthesize compounds **2** (Schemes 1 and 2), we applied a similar approach using 4 different 2-aminothiazole derivatives. The starting 2-aminotetrahydrobenzothiazole **1b** was obtained by reaction of cyclohexanone with thiourea in the presence of iodine, whereas the compounds 2-amino-5-benzyl-4,5,6,7-tetrahydrothiazolo[5,4-c]pyridine **1a**, 2-amino-benzothiazole **1c**, and 2-amino-5-benzyl-4,5,6,7-tetrahydrothiazolo[4,5-c]pyridine **1d** were commercially available. Reaction of compound **1** with 2-bromo-4′-nitroacetophenone in ethanol provided the corresponding nitro derivatives **2** by alkylation of the ring nitrogen and concomitant dehydration using EtOH or *i*-PrOH [35]. The use of a polar solvent secured the concomitant second step, whereas the use of toluene induces only the first step of the reaction. The reduction of the nitro group was secured with $SnCl_2$ in MeOH-HCl or with Fe-powder in the presence of H_2SO_4 to give the corresponding anilines **3** (synthesis of compound **3c** is exemplified in Scheme 1). The use of $SnCl_2$ induces the secondary introduction of a chlorine atom at position 3 of the tricyclic core. In particular, this was the case for the preparation of **3b** and **3c,** whose yield was lower than 50%.

Glycine, *R*- and *S*-alanine, β-alanine, *R*- and *S*-phenylalanine, *R*-cysteine and *S*-tyrosine were selected for the generation of compounds **4** (Scheme 3), and subsequently condensed with the tricyclic scaffolds. The methyl esters of these aminoacids were reacted with 4-methylphenyl-, 3,5-difluorophenyl-, 3,5-dimethylphenyl-, and 3,5-bis(trifluoromethyl)phenyl-acetic acids in the presence of DCC or DCI. In the case of cysteine the corresponding methyl ester and S-trityl derivative was used. The hydrolysis of the methyl esters (NaOH, MeOH, 1 h) took place without any significant racemization (^{1}H NMR by shift reagent) and permitted the subsequent condensation reaction to complete the structure of the designed compounds (Schemes 4 and 5).

The building block **3a** (Scheme 2) was used for the formation of four different compounds (**5a**–**d**) (Scheme 4) using HATU (yield 70–90%) or BOPCl (yield 45–70%) as dehydrating agents. The formation of **5d** required removal of the trityl group with TFA and Et_3SiH in CH_2Cl_2. The use of building blocks **3b**, **3c**, **3d**, and **3e** (Schemes 1 and 2) permitted the production of **6, 7a**–**j**, **8a**–**c**, and **7k**, respectively (Schemes 4 and 5). All the obtained compounds were stable as solids and in solution (DMSO, $CHCl_3$, MeOH). Their structures were confirmed on the basis of the NMR and MS spectra.

2.3. Biology

2.3.1. Identification of imidazo[2,1-b]benzothiazol-2-ylphenyl compounds as a new class of inhibitors blocking Met-triggered cell scattering and cell survival

We have previously shown that compounds can be efficiently screened and/or biologically validated for their inhibitory properties toward Met-triggered biological responses by using cell scattering assays [32]. In particular, MDCK epithelial cells acquire a “scattered phenotype” following stimulation by HGF, the Met ligand. The scattering response to HGF is impaired in the presence

of inhibitors targeting Met [32,36]. For these studies, SU11274 was used as a reference Met inhibitor [37]. Among 20 newly synthesized imidazo[2,1-*b*]benzothiazol-2-ylphenyl compounds (**Ia**), we found that **7a**, **7b, 7c**, **7d**, **7e**, **7h**, and **7k** (Scheme 5) elicited inhibitory activity on Met-triggered cell scattering. By evaluating the IC_{50} of the most active compounds, we found that **7c** and **7d** impaired Met-triggered cell scattering at concentrations comparable to SU11274 (**7c**: 0.171 μM; **7d**: 0.206 μM; SU11274: 0.152 μM; Fig. 3A and Supplementary Fig. 1). No toxic effects were observed at biologically active concentrations and only found when compounds were applied at doses 50–100 fold higher (data not shown). Further validations were obtained by testing **Ia** compounds on human MCF10A breast cells and similar inhibitory properties on Met-triggered scattering were observed (data not shown).

We next investigated the ability of **Ia** compounds to prevent Met-triggered survival of cancer cells. These studies were performed on human HepG2 hepatocellular carcinoma cells, whose tumorigenesis is Met-dependent, and on human GTL-16 gastric carcinoma cells, in which *c-met* gene amplification results in high Met protein levels leading to its over-activation in a ligand independent manner. As a consequence, GTL-16 cells are extremely aggressive, "Met-addicted" for survival, anchorage-independent growth, and tumor formation when injected into nude mice [38]. We found that compounds **7a**, **7c**, **7d**, and **7e** reduced survival of both HepG2 and GTL-16 cells in a dose-dependent manner (Fig. 3B and C, and Supplementary Fig. 2A). Notably, **Ia** compounds did not restrain survival of cancer cell lines, such as BT474 and MCF7-ErbB2 (Fig. 3D and E), which are addicted to ErbB oncogenes [39]. Altogether, these studies identified a new class of biologically active compounds characterized by a new moiety, namely imidazo[2,1-*b*]benzothiazol-2-ylphenyl, and displaying inhibitory effects on cells with activated Met.

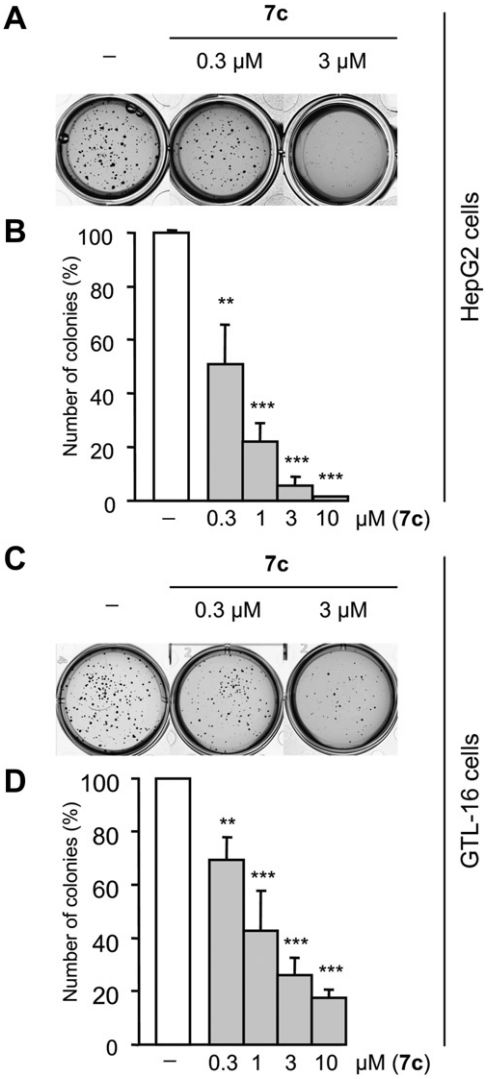

Fig. 4. Compound **7c** blocks in vitro tumorigenesis triggered by Met. **7c** impairs anchorage-independent growth of HepG2 (A and B) and GTL-16 (C and D) cells, in a dose dependent manner (μM; $n = 3$). Values are expressed as means ± s.e.m. $^{**}P < 0.01$; $^{***}P < 0.001$; Student-*t* test.

2.3.2. *Imidazo[2,1-b]benzothiazol-2-ylphenyl compounds interfere with Met-triggered in vitro tumorigenesis*

We next ascertained whether the identified **Ia** class of compounds also prevented Met-triggered anchorage-independent growth, a hallmark of oncogenic transformation. Soft-agar growth of HepG2 cells requires intact Met as it is restrained by the Met inhibitor SU11274 [38]. We found that compounds **7a**, **7c**, **7d**, and **7e** impaired in vitro tumorigenesis of HepG2 cells, in a dose dependent manner (Fig. 4A and B, and Supplementary Fig. 2B). By evaluating the IC_{50} of the most active compounds, we found that **7c** and **7d** interfered with Met-triggered anchorage-independent growth at concentrations 3–5 folds lower than those required for SU11274 (**7c**: 0.321 μM; **7d**: 0.620 μM; SU11274: 1.561 μM; Fig. 4A and B, Supplementary Figs. 2B and 3). Tumorigenesis of GTL-16 cells addicted to the Met oncogene was also blocked by **Ia** compounds, in a dose dependent manner (Fig. 4C and D, and Supplementary Fig. 2C). **7c** and **7d** were again the most active compounds (**7c**: 0.811 μM; **7d**: 1.194 μM; SU11274: 0.228 μM; Supplementary Fig. 3). Altogether, these findings demonstrate that **Ia** compounds restrain in vitro tumorigenesis of cells dependent or addicted to the Met oncogene. As **7c** appeared among the most effective compounds we have identified, its properties were further investigated through a series of in vitro and in vivo assays.

2.3.3. *Selectivity of imidazo[2,1-b]benzothiazol-2-ylphenyl compounds*

As several Met inhibitors additionally target other kinases, we tested **Ia** compound selectivity toward a panel of 16 Ba/F3 cells expressing the active form of different kinases. These studies were performed by following the proliferation of cells in the presence or absence of **7c** at concentrations ranging from 0.1 to 40 μM. As shown in Fig. 5, the **7c** compound at 1 μM interfered predominantly

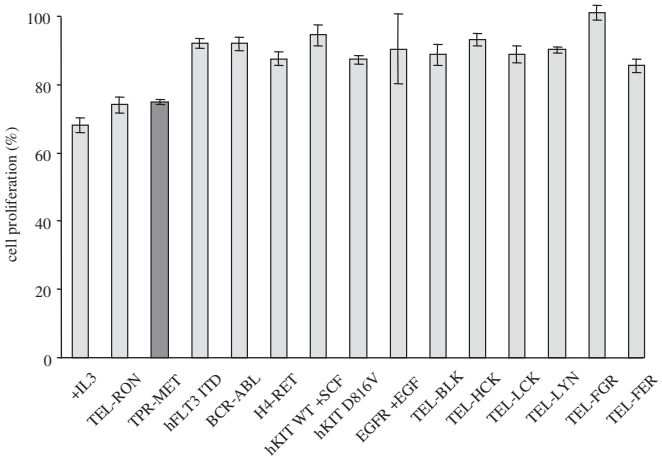

Fig. 5. Inhibition of BaF/3 cells transfected with active forms of the indicated kinases by compound **7c**. Cells were incubated in the presence of **7c** (1 μM) for 48 h before analyzing cell proliferation using Cell Titer Glo. Percentage represents proliferation of each cell line in the presence of **7c** compared to untreated cells.

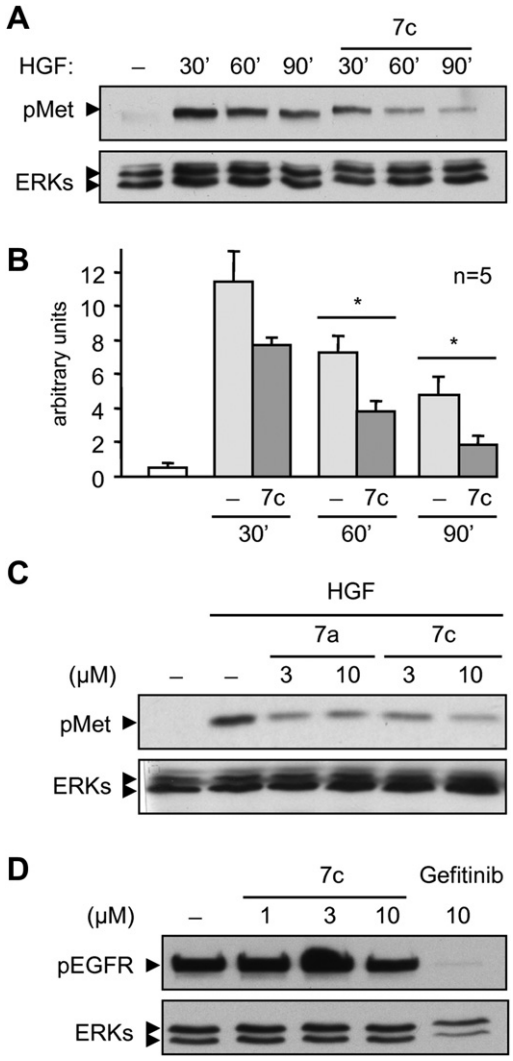

Fig. 6. Compound **7c** interferes with Met phosphorylation in living cells. (A) Met phosphorylation following HGF stimulation (20 ng/ml) in HepG2 cells was reduced in presence of **7c**. For western blot analyses, cells were treated with HGF for 30, 60, and 90 min in presence or not of **7c** (10 μM). Total cell lysates were analyzed using anti-phospho-Tyr1234/1235-Met (pMet) (upper panel). (B) Quantification of Met phosphorylation in presence or not of **7c** ($n = 5$). Values are expressed as means ± s.e.m. $^{*}P < 0.05$; Student-t test. (C) Met phosphorylation was also reduced by **7a** and **7c** applied at 3 and 10 μM in human MDA-MB231 breast cancer cells exposed to HGF stimulation for 15 min (D) **7c** does not affect EGFR phosphorylation in human BT-474 cells at 1, 3, and 10 μM concentrations. Gefitinib was used as positive control (10 μM). ERK protein levels were used as loading controls (lower panels in A, C, and D).

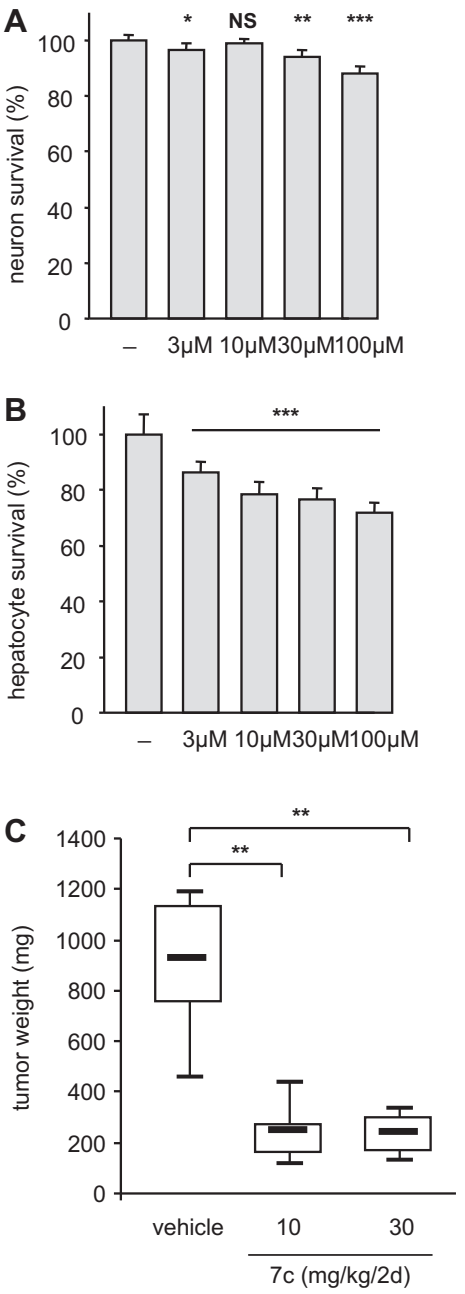

Fig. 7. Compound **7c** impairs in vivo tumor growth of cancer cells dependent on the Met oncogenic signaling, without eliciting major side effects either on primary neuron or hepatocyte cultures. (A and B) Survival of cortical neurons (A) and hepatocytes (B) was not drastically affected by **7c** (μM). For survival assays, cells were incubated with 7c for 24 h. (C) Compound **7c** interferes with growth of tumors triggered by cancer cells dependent on the Met oncogene. **7c** treatment (i.p. 10 or 30 mg kg^{-1} every 2 days) reduces tumor weight in nude mice injected intra-peritoneally with GTL-16 cells. Values are reported as boxplots. Two independent experiments were performed and 8 mice per group were used. Values are expressed as means ± s.e.m. $^{*}P < 0.05$; $^{**}P < 0.01$; Student-t test.

with proliferation of Ba/F3 cells expressing the oncogenic form of Met (TPR-Met), its family member Ron, or IL3. In this cellular system, the IC_{50} value of **7c** with regard to Met was 4 μM, which is higher than what was found when IC_{50} value was evaluated in HepG2 and GTL-16 cells. This difference could be due to the diversity in the biological assays and to the artifactual TPR-Met oncogenic form. Altogether, these studies establish that **Ia** compounds have a certain degree of selectivity toward inhibition of the Met-associated pathways in cells. Moreover, the inhibitory effects on Ba/F3 cells with IL3 suggest that they may also act on other RTK-distinct signaling molecules.

*2.3.4. Compound **7c** interferes with Met phosphorylation in living cells and with Met activation in vitro*

We next biochemically evaluated the ability of **Ia** compounds to interfere with Met activation by following the phosphorylation levels of two Tyrosine residues located in its kinase domain, namely Tyr1234 and Tyr1235. High levels of phospho-Met were observed upon HGF stimulation in HepG2 cells, which progressively decreased over time (Fig. 6A and B). Met phosphorylation was reduced by **7c** by 30–50% over time when compared to controls (Fig. 6A and B). Reduced Met phosphorylation by **7c** was also observed in other cell lines, such as in human MDA-MB231 breast cancer cells exposed to HGF stimulation (Fig. 6C). In contrast, **7c** did not interfere with phosphorylation of ErbB1 when applied to BT474 cells (Fig. 6D).

We next assessed the effects of **7c** on Met activation by using the Kinexus compound profiling service. This strategy determines the profile inhibition of a compound against protein kinases and protein phosphatase targets. The profiling data against Met revealed that **7c** restrains Met activation by 21 and 53% at 1 and 10 μM, respectively. As suggested by computer modeling and biological assays, these findings identify the new **Ia** scaffold as inhibitors of the Met RTK.

2.3.5. Compound **7c** impairs in vivo tumor growth of cancer cells dependent on the Met oncogene, without eliciting in vitro and in vivo side effects

To have a first indication of tolerance to compound **7c** for therapeutic use, we assessed its side effects on primary cultures of neurons and hepatocytes. Interestingly, compound **7c** was very well tolerated by both primary cells, leading to only a modest loss of cell viability even at high doses of 100 μM (neuron: 12% reduction; hepatocytes: 28% reduction; Fig. 7A and B).

Finally, the ability of **7c** to impair tumor growth of cancer cells dependent on Met oncogenic signaling was evaluated in vivo using xenograft nude mice as tumor initiation models. For these studies, GTL-16 cells were chosen for their dependency to the oncogenic Met signaling, leading to aggressiveness and resistance to chemotherapeutic agents. GTL-16 cells (10^6) were intra-peritoneally injected into nude mice and tumor growth was examined in mice treated with **7c** or vehicle alone. Intra-peritoneal injection of cancer cells leads to development of several nodules in the peritoneal cavity, offering the possibility to evaluate compound efficacy on tumor weight. Notably, we found that the tumor weight was drastically reduced in mice injected with **7c** tested at different doses (Fig. 7C). In particular, when **7c** was administered to mice at a dose of 10 or 30 mg kg^{-1} every other day, we found 70% reduction in tumor weight (control: 865.4 ± 348.9; **7c** injected 10 mg kg^{-1}: 268.8 ± 159.7, $P = 0.002$; **7c** injected 30 mg kg^{-1}: 234.8 ± 88.5, $P = 0.001$; Fig. 7C). No major side effects were observed, evaluated by following the weight of mice treated with **7c** (data not shown). Taken together, these findings demonstrate that in vivo **7c** elicits tumor growth inhibition of cancer cells dependent on the Met oncogene. Moreover, the absence of side effects neither in neurons and hepatocytes nor in vivo indicates that **7c** is well tolerated when injected into mice at doses required to elicit its anti-tumor effects.

3. Conclusion

The discovery that RTKs might be targeted by chemical agents at different sites in their conformational space has generated great hope for molecularly targeted anticancer therapies. Previous studies have shown that Met is a particularly attractive target in this regard [28]. Indeed, the triple-binding-mode capacity of the Met RTK can be exploited to identify new agents with inhibitory properties toward cancer cells addicted to oncogenic Met signaling. Our findings show how support from computer-aided drug design could be useful to medicinal chemistry investigations. An integrated interdisciplinary screening strategy, based on rational drug design coupled to a cell-based focused screen and supported by molecular modeling from existing crystallographic complexes, led us to identify aminoacid amides containing the imidazo[2,1-*b*]benzothiazol-2-ylphenyl moiety **Ia** as new effective agents targeting Met-driven tumorigenesis. In particular, the biological evaluation of these agents in living cells allowed us to directly assess their inhibitory properties toward oncogenic Met signaling while excluding compounds causing side effects, leading to the identification of those exerting anti-tumorigenic activity in xenograft models.

Notably, as the identified imidazo[2,1-*b*]benzothiazol-2-ylphenyl derivatives have been screened in cultured cancer cells addicted to the Met oncogene, they may act on signals required to execute the Met-driven oncogenic program, in addition to targeting the Met RTK directly. This possibility is well supported by our previous studies showing that the tetrahydrobenzothiazole scaffold impairs Met signaling and also prevents Met restoration after degradation [32]. Our cell-based selectivity assays show that the identified **Ia** compounds predominantly target Met family members rather than other RTKs, which are impaired by Met inhibitors previously discovered [31,37,38,40–42]. Intriguingly, the most active imidazo [2,1-*b*]benzothiazol-2-ylphenyl derivative interferes with anchorage-independent growth of HepG2 cells at lower concentrations than those required for SU11274. Instead, GTL-16 cells are slightly more sensitive to SU11274 inhibition rather than to imidazo [2,1-*b*]benzothiazol-2-ylphenyl derivatives. This might reflect their inhibitory properties according to the level of activated Met. Alternatively, their efficacy may depend on the sets of signals activated by oncogenic Met, which vary between cancer cells and is paralleled by their differential sensitiveness to the action of compounds. Future studies will further establish the drug action of **Ia** compounds and their effectiveness toward a panel of different cancer cells to fully exploit their anticancer properties for single or combined therapies.

4. Experimental protocols

4.1. Computational part

4.1.1. Representation of molecular structures

ChemDraw 6.0 was used to represent the 2D structures. Pymol (DeLano Scientific LLC) and GNU Image Manipulation Program (GIMP 2.6) were used for generating the 3D representations.

4.1.2. Docking simulations

Docking calculations were done with GOLD v4.0 (CCDC) [43–45]. The Kinase Scoring function was chosen. This ChemScore variant aims at better assessing weak H-bonds by adding specific terms relevant to the kinase inhibitors' signature N-heterocycle/CH…O interactions. The automatic generic algorithm settings of GOLD were employed using the search efficiency set to 100%, and the number of docking runs per ligand set to 30. The binding site was defined within 5 Å of the cocrystallized ligands coordinates. The Met receptor structures were prepared (protonation, modeling of missing elements) from the original PDB files using Maestro v8.5 (Schrödinger). Starting structures of inhibitors were built using Maestro 3D-sketcher then minimized with the OPLS_2005 force field [46] using the Polak-Ribiere conjugated gradient method (0.001 kJ/Å·mol convergence). The reliability of the docking protocol was tested by retrieving the binding mode of Met inhibitors as cocrystallized in the 2RFS, 3CTJ, and 3EFK PDB X-ray structures, giving a negligible deviation from the crystallographic-resolved positions (RMSD < 1 Å) in all cases.

4.2. Chemistry

4.2.1. General

Melting points were determined in a capillary tube on a Büchi apparatus and are uncorrected. NMR spectra were recorded at 200, 300, 400 or 500 MHz (^{1}H) and 75.4, 100.6 or 125.9 MHz (^{13}C). Chemical shifts are reported in δ values downfield from TMS. IR spectra were recorded on a Perkin–Elmer 1600 spectrophotometer and only noteworthy IR absorptions are listed. Optical rotations were measured on a Perkin–Elmer 241 polarimeter using a 1 dm cell with a total volume of 1 ml. EI mass spectra were recorded at an ionizing voltage of 6 KeV on a VG 70-70 EQ. ESI mass spectra were recorded on FT-ICR APEX^{II} (Bruker Daltonics). High resolution mass spectra (HMRS; LC/MSD TOF Agilent Technologies) were performed by *Serveis Científico-Tècnics*, Barcelona. Thin-layer chromatography

was done on SiO_2 (silica gel 60 F_{254}, Merck), and the spots were located with UV light or aqueous potassium permanganate solution. Flash chromatoghraphy was carried out using SiO_2 (silica gel 60, SDS, 35–70 μ). All nonaqueous reactions were performed under an inert atmosphere. Solvents for chromatography were distilled at atmospheric pressure prior to use and dried using standard procedures. Drying of the organic extracts during the workup of reactions was performed over anhydrous Na_2SO_4 or $MgSO_4$. Evaporation of solvents was accomplished with a rotatory evaporator. Elemental analyses were performed by *Centre d'Investigació i Desenvolupament* (CSIC). All test compounds showed >95% purity as determined by combustion analysis.

4.2.2. 2-Amino-4,5,6,7-tetrahydrobenzothiazole (**1b**)

A mixture of cyclohexanone (3.0 g, 30.6 mmol), thiourea (4.65 g, 61.1 mmol) and iodine (7.76 g, 30.6 mmol) was stirred at 110 °C for 12 h. The reaction mixture was cooled to room temperature. Hot water was then added and the resulting solution was stirred for 30 min. The aqueous solution was washed with diethyl ether and then neutralized by the addition of solid $NaHCO_3$. The pale yellow crystals were collected by filtration. The hydroiodide salt was dissolved in a hot saturated aqueous solution of Na_2CO_3. After cooling, the aqueous solution was extracted with CH_2Cl_2. The organic layer was dried over anhydrous Na_2SO_4, filtered, and concentrated under reduced pressure. The compound **1b** was obtained without any further purification as pale yellow solid (3.39 g, 72%). ^{1}H NMR (DMSO-d_6 300 MHz) δ 6.61 (2H, s), 2.52–2.48 (2H, m), 2.38–2.35 (2H, m), 1.72–1.68 (4H, m). MS-EI m/z $[M]^+$ 154.

4.2.3. 2-Amino-6-bromo-2-benzothiazole (**1e**)

A solution of 4-bromoaniline (0.500 g, 2.91 mmol) and potassium thiocyanate (1.13 g, 11.6 mmol) in AcOH (10 ml) was stirred at 20 °C for 10 min. Bromine (150 μl, 2.91 mmol) was added over 20 min to the above solution. The reaction mixture was stirred further at room temperature for 60 min. On completion of reaction following a TLC examination, the reaction mixture was poured into a solution of NH_3 5M and extracted with AcOEt. The organic layer was dried over anhydrous Na_2SO_4 and concentrated under reduced pressure. The crude product obtained was purified by flash chromatography (Hex:AcOEt 1:1) to afford **1e** as white solid (2.67 g, yield 79%). ^{1}H NMR (DMSO-d_6, 400 MHz): δ 7.91 (1H, d, J = 2.5 Hz), 7.63 (2H, s), 7.35 (1H, dd, J = 11.6, 2.5 Hz), 7.26 (1H, d, J = 11.6 Hz). MS-EI m/z $[M]^+$ 228.

4.2.4. General procedure for synthesis of (**2**)

A mixture of **1** (4 mmol) and 2-bromo-4′-nitroacetophenone (4.4 mmol) was refluxed in EtOH or *i*-PrOH (6–10 ml) for 50–90 min, the mixture was cooled to 0 °C. The solid was collected by filtration and washed with ethanol to afford **2** without any further purification.

4.2.5. 7-Benzyl-2-(4-nitrophenyl)-5,6,7,8-tetrahydroimidazo [2′,1′:2,3]thiazolo[5,4-c]pyridine (**2a**)

2-amino-5-benzyl-4,5,6,7-tetrahydrothiazolo[5,4-*c*]pyridine (**1a**, 1.0 g, 4.08 mmol) and 2-bromo-4′-nitroacetophenone (1.09 g, 4.49 mmol) were dissolved in *i*-PrOH (6 ml). **2a** (1.67 g, 41%), pale yellow solid. ^{1}H NMR ($CDCl_3$, 400 MHz): δ 8.22 (2H, d, J = 8.8 Hz), 7.94 (2H, d, J = 8.8 Hz), 7.70 (1H, s), 7.27–7.37 (5H, m), 3.78 (2H, s), 3.61 (2H, s), 3.01 (2H, t, J = 6.0 Hz), 2.81 (2H, t, J = 6.0 Hz). MS-EI m/z $[M]^+$ 390.

4.2.6. 2-(4-Nitrophenyl)-5,6,7,8-tetrahydroimidazo[2,1-b] benzothiazole (**2b**) [47]

1b (3.00 g, 19.5 mmol) and 2-bromo-4′-nitroacetophenone (5.24 g, 21.4 mmol). **2b** (2.31 g, yield 40%), yellow solid. ^{1}H NMR (DMSO-d_6, 300 MHz): δ 8.52 (1H, s), 8.27 (2H, d, J = 8.8 Hz), 8.09 (2H, d, J = 8.8 Hz), 2.73–2.69 (4H, m), 1.92–1.88 (4H, m); MS-EI m/z $[M]^+$ 299.

4.2.7. 2-(4-Nitrophenyl)imidazo[2,1-b]benzothiazole (**2c**) [48]

2-Aminobenzothiazole (**1c**, 1.00 g, 6.4 mmol) and 2-bromo-4′-nitroacetophenone (1.83 g, 7.1 mmol). **2c** (495 mg, yield 26%) yellow solid. ^{1}H NMR (DMSO-d_6, 300 MHz): δ 9.10 (1H, s), 8.34 (2H, d, J = 9.0 Hz), 8.12 (2H, d, J = 9.0 Hz), 8.07 (1H, d, J = 8.0 Hz), 8.02 (1H, d, J = 8.0 Hz), 7.64 (1H, t, J = 8.0 Hz), 7.49 (1H, t, J = 8.0 Hz). MS-EI m/z $[M]^+$ 295.

4.2.8. 6-Benzyl-2-(4-nitrophenyl)-5,6,7,8-tetrahydroimidazo [2′,1′:2,3]thiazolo[4,5-c]pyridine (**2d**)

2-Amino-5-benzyl-4,5,6,7-tetrahydrothiazolo[4,5-*c*]pyridine (**1d**, 3.9 g, 16.1 mmol) and 2-bromo-4′-nitroacetophenone (4.7 g, 19.4 mmol) in *i*-PrOH (80 ml). **2d** (2.28 g, 45%) was directly submitted to the next step without further purification.

4.2.9. 7-Bromo-2-(4-nitrophenyl)imidazo[2,1-b]bromobenzole (**2e**)

A mixture of **21** (1.20 g, 5.24 mmol) and 2-bromo-4′-nitroacetophenone (1.41 g, 5.76 mmol) was refluxed in ethanol for 90 min, the mixture was cooled to 0 °C. The solid was collected by filtration and washed with ethanol to afford **2e** without any further purification. Yellow solid (0.665 g, yield 34%). ^{1}H NMR (DMSO-d_6, 400 MHz, 80 °C): δ 8.92 (1H, s), 8.32 (1H, d, J = 1.9 Hz), 8.28 (2H, d, J = 8.8 Hz), 8.12 (2H, d. J = 8.8 Hz), 7.96 (1H, d, J = 8.6 Hz), 7.76 (1H, dd, J = 8.6, 1.9 Hz). ^{13}C NMR (DMSO-d_6 100.6 MHz) 80 °C: δ155.67, 146.92, 145.02, 140.78, 132.15, 131.47, 130.15, 127.93, 125.93 (2C), 124.62 (2C), 117.76, 115.53, 112.47. MS-EI $[M]^+$ 373.

4.2.10. General procedure for synthesis of (**3**)

Procedure A: Fe (powder, 7 g) and H_2SO_4 (12 N, 0.7 ml) were added to a solution of **2** (6 mmol) in ethanol/water (5:1, 50–100 ml) and the mixture was stirred at 90 °C for 1 h. The hot solution was filtered through celite and washed with hot ethanol. The solvent was removed in vacuo and the crude material was extracted by satured solution of $NaHCO_3$ and AcOEt. The organic phase was dried with Na_2SO_4 anhydrous. Compound **3** was obtained without any further purification. *Procedure B:* HCl (37%, 100 ml) was slowly added to a mixture of **2** (3.4 mmol) and $SnCl_2$ (13 mmol) in MeOH (100 ml). The crude mixture was refluxed for 30 min. A solution of K_2CO_3 (2M) was slowly added to reach pH 9. The precipitate was filtered and purified by flash chromatography.

4.2.11. 2-(4-Aminophenyl)-7-benzyl-5,6,7,8-tetrahydroimidazo [2′,1′:2,3]thiazolo[5,4-c]pyridine (**3a**)

From crude **2a** using the procedure B. Flash chromatography (AcOEt + 0.1% NEt_3). **3a** (26%), pale yellow solid. ^{1}H NMR ($CDCl_3$, 400 MHz): δ 7.60 (2H, d, J = 8.4 Hz), 7.39 (1H, s), 7.25–7.36 (5H, m), 6.69 (2H, d, J = 8.4 Hz), 3.73 (2H, s), 3.56 (2H, s), 2.95 (2H, t, J = 6.0 Hz), 2.71 (2H, t, J = 6.0 Hz). MS-EI m/z $[M]^+$ 360.

4.2.12. 2-(4-Aminophenyl)-5,6,7,8-tetrahydroimidazo[2,1-b] benzothiazole (**3b**)

From crude **2b** using the procedure A. **3b** (89%), yellow solid. ^{1}H NMR (DMSO-d_6, 300 MHz): δ 7.87 (1H, s), 7.50 (2H, d, J = 8.2 Hz), 6.58 (2H, d, J = 8.2 Hz), 5.13 (2H, s), 2.69–2.64 (4H, m), 1.89–1.85 (4H, m). MS-EI m/z $[M]^+$ 269.

4.2.13. 2-(4-Aminophenyl)imidazo[2,1-b]benzothiazole (**3c**)

From crude **2c** using the procedure A. **3c** (87%), pale yellow amorphous solid. ^{1}H NMR (DMSO-d_6, 300 MHz): δ 8.48 (1H, s), 8.05 (1H, d, J = 8.0 Hz), 7.93 (1H, d, J = 8.0 Hz), 7.61–7.51 (3H, m), 7.42 (1H, t, J = 8.0 Hz), 6.64 (2H, d, J = 9.0 Hz), 5.23 (2H, s). MS-EI m/z $[M]^+$ 265.

4.2.14. 2-(4-Aminophenyl)-6-benzyl-5,6,7,8-tetrahydroimidazo [2′,1′:2,3]thiazolo[4,5-c]pyridine (**3d**)

From **2d** using the procedure B. Flash chromatography (CH_2Cl_2 to CH_2Cl_2/MeOH = 98.5:1.5). **3d** (23%). R_f (CH_2Cl_2/MeOH = 95/5):

0.18 .^{1}H NMR ($CDCl_3$ with drops of CD_3OD, 400 MHz) δ 7.52 (2H, d, J = 8.8 Hz), 7.33–7.39 (5H, m), 6.73 (2H, d, J = 8.8 Hz), 3.80 (2H, s), 3.57 (2H, t(dd), J = 1.5 Hz), 2.95 (2H, t(dd), J = 5.2 Hz), 2.82 (2H, t(dd), J = 5.2 Hz). ^{13}C NMR ($CDCl_3$ with drops of CD_3OD, 100.6 MHz) δ 148.2, 146.6, 145.7, 136.8, 128.8 (2C), 128.3 (2C), 127.4, 125.9 (2C), 124.2, 124.0, 119.3, 115.2 (2C), 104.1, 61.4, 49.9, 48.8, 24.2. HRMS calcd for $C_{21}H_{21}N_4S$ $[M + H]^+$: 361.1487; Found: 361.1480.

4.2.15. 2-(4-Aminophenyl)-7-bromoimidazo[2,1-b]benzothiazole (**3e**)

From **2e** using the procedure A. **3e** (92%), amorphous brown solid. ^{1}H NMR (DMSO-d_6, 400 MHz): δ 8.46 (1H, s), 8.31 (1H, d, J = 1.9 Hz), 7.89 (1H, d, J = 8.6 Hz), 7.73 (1H, dd, J = 8.6, 1.9 Hz), 7.53 (2H, d, J = 8.5 Hz), 6.62 (2H, d, J = 8.5 Hz), 5.21 (2H, s). ^{13}C NMR (DMSO-d_6, 100.6 MHz): δ 149.41, 149.07, 147.41, 132.39, 132.35, 130.52, 128.41, 126.94 (2C), 122.78, 117.31, 115.67, 115.08 (2C), 107.58. HR-EIMS calcd for $[C_{15}H_{10}BrN_3S]^+$ 342.9779; Found 342.9784.

4.2.16. General procedure for synthesis of (**4**)

Procedure A: A solution of a phenylacetic acid (3.7 mmol), DMAP (5.55 mmol) and DCC (5.55 mmol) in THF (40–70 ml) was stirred at room temperature (rt) for 30 min. The hydrochloride salt of the carboxy protected aminoacid (3.7 mmol) was added and the solution was stirred for 48 h at rt. The crude mixture was filtered over celite and the solvent was removed in vacuo. The product was purified by flash chromatography. The methyl ester (1eq) was dissolved in methanol. A solution of NaOH (1N, 17 ml) was added and the reaction mixture was stirred for 1 h at rt. H_2O was added and methanol only was evaporated under reduced pressure. The pH was reduced to 2 using HCl solution 1N. The crude material was extracted with ethyl acetate and the organic phase was dried with Na_2SO_4 anhydrous. The solvent was removed in vacuo to afford **4** without any further purification. *Procedure B*: A solution of phenylacetic acid (6 mmol), the hydrochloride salt of the carboxy protected aminoacid (6 mmol), DMAP (3 mmol) and DCI (10 mmol) in (50–80 ml) was stirred at r.t. for 14 h. The crude mixture was filtered over celite and the solvent was removed in vacuo. The product was purified by flash chromatography. Treatment with NaOH as reported in procedure A.

4.2.17. (S)-2-[2-(3,5-Dimethylphenyl)acetamido]-3-phenylpropanoic acid (**4a**)

From L-phenylalanine methyl ester hydrochloride and 3,5-dimethylphenylacetic acid with procedure A. Flash chromatography (Hex:AcOEt 2:1) to afford the methyl ester as white solid (70%). ^{1}H NMR ($CDCl_3$, 400 MHz): δ 7.24–7.18 (3H, m), 6.94–6.91 (3H, m), 6.82 (2H, s), 5.83 (1H, d, J = 7.6 Hz), 4.91–4.83 (1H, m), 3.66 (3H, s), 3.52 (1H, d, J = 15.8 Hz), 3.48 (1H, d, J = 15.8 Hz), 3.09 (1H, dd, J = 13.8, 5.5 Hz), 3.04 (1H, dd, J = 13.8, 5.5 Hz), 2.19 (6H, s). MS-EI m/z $[M]^+$ 325. The NaOH treatment gave **4a** (95%), white solid. mp 85–88 °C, $[\alpha]_D^{20}$ = +35.12 (c 0.80, $CHCl_3$). ^{1}H NMR ($CDCl_3$, 400 MHz): δ 10 (1H, s), 7.24–7.19 (3H, m), 6.97 (2H, dd, J = 7.2, 1.6 Hz), 6.94 (1H, s), 6.78 (2H, s), 6.01 (1H, d, J = 7.6 Hz), 4.87–4.83 (1H, m), 3.52 (1H, d, J = 16.4 Hz), 3.48 (1H, d, J = 16.4 Hz), 3.16 (1H, dd, J = 14.0, 5.6 Hz), 3.06 (1H, dd, J = 14.0, 5.6 Hz), 2.3 (6H, s). ^{13}C NMR ($CDCl_3$, 100.6 MHz): δ 174.4, 172.2, 138.6 (2C), 135.4, 133.7, 129.7, 129.2 (2C), 128.5 (2C), 127.3 (2C), 127.1, 53.2, 43.2, 36.9, 21.2 (2C). HR-EIMS calcd for $C_{19}H_{21}NO_3$ 311.1521. Found 311.1523.

4.2.18. (R)-2-[2-(3,5-Dimethylphenyl)acetamido]-3-phenylpropanoic acid (**4b**)

From D-phenylalanine methyl ester hydrochloride and 3,5-dimethylphenylacetic acid with procedure A. Flash chromatography (Hex:AcOEt 2:1) to afford the methyl ester (68%) as white solid. ^{1}H NMR ($CDCl_3$, 400 MHz): δ 7.24–7.18 (3H, m), 6.94–6.91 (3H, m), 6.82 (2H, s), 5.83 (1H, d, J = 7.6 Hz), 4.91–4.83 (1H, m), 3.66 (3H, s), 3.52 (1H, d, J = 15.8 Hz), 3.48 (1H, d, J = 15.8 Hz), 3.09 (1H, dd, J = 13.8, 5.5 Hz), 3.04 (1H, dd, J = 13.8, 5.5 Hz), 2.19 (6H, s). MS-EI m/z $[M]^+$ 325. The NaOH treatment gave **4b** (98%), white solid. mp 85–88 °C, $[\alpha]_D^{20}$ = −38.52 (c 1.28, $CHCl_3$). ^{1}H NMR ($CDCl_3$, 400 MHz): δ 10 (1H, s), 7.24–7.19 (3H, m), 6.97 (2H, dd, J = 7.2, 1.6 Hz), 6.94 (1H, s), 6.78 (2H, s), 6.01 (1H, d, J = 7.6 Hz), 4.87–4.83 (1H, m), 3.52 (1H, d, J = 16.4 Hz), 3.48 (1H, d, J = 16.4 Hz), 3.16 (1H, dd, J = 14.0, 5.6 Hz), 3.06 (1H, dd, J = 14.0, 5.6 Hz), 2.3 (6H, s). ^{13}C NMR ($CDCl_3$, 100.6 MHz): δ 174.4, 172.2, 138.6 (2C), 135.4, 133.7, 129.7, 129.2 (2C), 128.5 (2C), 127.2 (2C), 127.1, 53.2, 43.2, 36.9, 21.2 (2C). HR-EIMS calcd for $C_{19}H_{21}NO_3$ 311.1521. Found 311.1526.

4.2.19. (S)-2-[2-(3,5-Bis(trifluoromethyl)phenyl)acetamido]-3-phenylpropanoic acid (**4c**)

From L-phenylalanine methyl ester hydrochloride and 3,5-bis(trifluoromethyl)phenylacetic acid with procedure A. Flash chromatography (Hex:AcOEt 2:1) to afford the methyl ester (63%), white solid. ^{1}H NMR ($CDCl_3$, 400 MHz): δ 7.82 (1H, s), 7.72 (2H, s), 7.27–7.23 (3H, m), 7.01–6.98 (2H, m), 5.97 (1H, d, J = 7.2 Hz), 4.93–4.88 (1H, m), 3.79 (3H, s), 3.66 (1H, d, J = 15.6 Hz), 3.61 (1H, d, J = 15.6 Hz), 3.17 (1H, dd, J = 13.6, 5.6 Hz), 3.09 (1H, dd, J = 13.6, 5.4 Hz). MS-EI m/z 433 $[M]^+$. The treatment with NaOH gave **4c** (99%) as white solid. mp 138–140 °C, $[\alpha]_D^{20}$ = +10.17 (c 1.28, MeOH). ^{1}H NMR (DMSO-d_6, 400 MHz): δ 8.52 (1H, d, J = 8.2 Hz), 7.96 (1H, s), 7.88 (2H, s), 7.22–7.13 (5H, m), 4.49–4.43 (1H, m), 3.65 (1H, d, J = 15.3 Hz), 3.57 (1H, d, J = 15.3 Hz), 3.09 (1H, dd, J = 13.8, 4.6 Hz), 2.86 (1H, dd, J = 13.8, 9.8 Hz).^{13}C NMR (DMSO-d_6, 100.6 MHz): δ 173.9, 169.9, 140.7, 138.5, 131.1 (2C, q, J = 32.8 Hz), 130.9 (2C), 130.1 (2C), 129.1 (2C), 127.4, 124.5 (2C, q, J = 272.6 Hz), 121.2, 54.6, 42.2, 37.9. HR-EIMS calcd. for $C_{19}H_{15}F_6NO_3$ 419.0956. Found 491.0952.

4.2.20. (R)-2-[2-(3,5-Bis(trifluoromethyl)phenyl)acetamido]-3-phenylpropanoic acid (**4d**)

From D-phenylalanine methyl ester hydrochloride and 3,5-bis(trifluoromethyl)phenylacetic acid with procedure A. Flash chromatography (Hex:AcOEt 2:1) to afford the methyl ester as white solid (62%). ^{1}H NMR ($CDCl_3$, 400 MHz): δ 7.82 (1H, s), 7.72 (2H, s), 7.27–7.23 (3H, m), 7.01–6.98 (2H, m), 5.97 (1H, d, J = 7.2 Hz), 4.93–4.88 (1H, m), 3.79 (3H, s), 3.66 (1H, d, J = 15.6 Hz), 3.61 (1H, d, J = 15.6 Hz), 3.17 (1H, dd, J = 13.6, 5.6 Hz), 3.09 (1H, dd, J = 13.6, 5.4 Hz). MS-EI m/z $[M]^+$ 433. The treatment with NaOH gave **4d** (99%), white solid. mp 138–140 °C, $[\alpha]_D^{20}$ = +10.5 (c 0.21, MeOH). ^{1}H NMR (DMSO-d_6, 400 MHz): δ 8.52 (1H, d, J = 8.2 Hz), 7.96 (1H, s), 7.88 (2H, s), 7.22–7.13 (5H, m), 4.49–4.43 (1H, m), 3.65 (1H, d, J = 15.3 Hz), 3.57 (1H, d, J = 15.3 Hz), 3.09 (1H, dd, J = 13.8, 4.6 Hz), 2.86 (1H, dd, J = 13.8, 9.8 Hz).^{13}C NMR (DMSO-d_6, 100.6 MHz): δ 173.8, 169.9, 140.7, 138.5, 131.1 (2C, q, J = 32.8 Hz), 130.9 (2C), 130.1 (2C), 129.1 (2C), 127.4, 124.5 (2C, q, J = 272.6 Hz), 121.2, 54.6, 42.1, 37.9. HR-EIMS calcd for $C_{19}H_{15}F_6NO_3$ 419.0955. Found 491.0952.

4.2.21. (S)-2-[2-(3,5-Difluorophenyl)acetamido]-3-phenylpropanoic acid (**4e**)

From L-phenylalanine methyl ester hydrochloride and 3,5-difluorophenylacetic acid with procedure A. Flash chromatography (Hex:AcOEt 2:1) to afford the methyl ester as white solid (75%). ^{1}H NMR ($CDCl_3$, 300 MHz): δ 7.25–7.23 (3H, m), 6.96–6.92 (2H, m), 6.74–6.70 (3H, m), 5.83 (1H, d, J = 6.8 Hz), 4.88–4.82 (1H, m), 3.73 (3H, s), 3.50 (1H, d, J = 14.2 Hz), 3.47 (1H, d, J = 14.2 Hz), 3.12 (1H, dd, J = 13.8, 5.6 Hz), 3.02 (1H, dd, J = 13.8, 5.9 Hz). MS-EI m/z 333 $[M]^+$. The treatment with NaOH gave **4e** (91%) as white solid. mp 182–184 °C, $[\alpha]_D^{20}$ = +33.63 (c 0.96, MeOH:$CHCl_3$ = 1:1). ^{1}H NMR (DMSO-d_6, 400 MHz): δ 8.48 (1H, d, J = 8.2 Hz), 7.26–7.18 (5H, m), 7.09–7.03 (1H, m), 6.87–6.83 (2H, m), 4.48–4.42 (1H, m),

3.49 (1H, d, J = 14.2 Hz), 3.43 (1H, d, J = 14.2 Hz), 3.09 (1H, dd, J = 13.8, 4.7 Hz), 2.86 (1H, dd J = 13.8, 9.8 Hz). ^{13}C NMR (DMSO-d_6, 100.6 MHz): δ 173.4, 169.4, 162.5 (2C, dd, J = 245.5, 14.1 Hz), 140.9 (t, J = 10.0 Hz), 137.9, 129.5 (2C), 128.5 (2C), 126.8, 112.6 (2C, d, J = 25.2 Hz), 102.2 (2C, t, J = 25.2 Hz), 53.9, 41.8, 37.1. HR-EIMS calcd for $C_{17}H_{15}F_2NO_3$ 319.1020. Found 319.1019.

4.2.22. 2-[2-(3,5-Dimethylphenyl)acetamido]acetic acid (**4f**)

From glycine methyl ester hydrochloride and 3,5-dimethylphenylacetic acid with procedure A. Flash chromatography (Hex:AcOEt 2:3) gave the methyl ester as white solid (52%). ^{1}H NMR ($CDCl_3$, 300 MHz): δ 6.92 (1H, s), 6.88 (2H, s), 5.92 (1H, d, J = 5.1 Hz), 3.99 (2H, d, J = 5.1 Hz), 3.72 (3H, s), 3.54 (2H, s), 2.30 (6H, s). MS-EI m/z 235 $[M]^+$. Treatment with NaOH gave **4f** (95%) as white solid. mp 129–131 °C ^{1}H NMR (DMSO-d_6, 400 MHz): δ 8.30 (1H, t, J = 5.7 Hz), 6.88, (2H, s), 6.85 (1H, s), 3.75 (2H, d, J = 5.7 Hz), 3.39 (2H, s), 2.23 (6H, s). ^{13}C NMR (DMSO-d_6, 100.6 MHz): δ 171.7, 171.0, 137.5 (2C), 136.4, 128.2, 127.3 (2C), 42.3, 41.2, 21.3 (2C). HR-EIMS calcd for $C_{12}H_{15}NO_3$ 221.1051. Found 221.1053.

4.2.23. (S)-2-[2-(3,5-Dimethylphenyl)acetamido]-3-(4-hydroxyphenyl)propanoic acid (**4g**)

From L-tyrosine methyl ester hydrochloride and 3,5-dimethylphenylacetic acid with procedure A. Flash chromatography (Hex:AcOEt 2:3) gave the methyl ester as white solid (43%). ^{1}H NMR ($CDCl_3$, 400 MHz): δ 7.12–7.05 (3H, m), 6.80–6.78 (2H, m), 6.69 (2H, d, J = 9.0 Hz), 5.71 (1H, d, J = 7.6 Hz), 4.85–4.79 (1H, m), 3.53 (3H, s), 3.41 (1H, d, J = 15.7 Hz), 3.34 (1H, d, J = 15.7 Hz), 2.98 (1H, dd, J = 13.8, 5.8 Hz), 2.96 (1H, dd, J = 13.8, 5.8 Hz), 2.07 (6H, s). MS-EI m/z 341 $[M]^+$. The treatment with NaOH gave **4g** (97%) as white solid. mp 145–148 °C, $[\alpha]_D^{20}$ = +22.0 (c 1.35, MeOH). ^{1}H NMR ($CDCl_3$, 400 MHz): δ 7.12–7.07 (3H, m), 6.91 (2H, dd, J = 7.1, 1.7 Hz), 6.68 (2H, d, J = 9.01 Hz), 5.86 (1H, d, J = 7.6 Hz), 4.91–4.85 (1H, m), 3.59 (1H, d, J = 16.4 Hz), 3.51 (1H, d, J = 16.4 Hz), 3.23 (1H, dd, J = 14.0, 5.6 Hz), 3.06 (1H, dd, J = 14.0, 5.6 Hz), 2.3 (6H, s). ^{13}C NMR ($CDCl_3$, 100.6 MHz): δ 174.3, 172.2, 155.6, 138.6 (2C), 133.7, 130.3, 129.7, 129.4 (2C), 127.3 (2C), 115.7 (2C), 53.2, 43.2, 36.9, 21.2 (2C). EIMS m/z 327 (M^+).

4.2.24. 3-[2-(3,5-Difluorophenyl)acetamido]propanoic acid (**4h**)

From β-alanine methyl ester hydrochloride and 3,5-difluorophenylacetic acid with procedure B. Flash chromatography (hexane/ethyl acetate 2:3) gave the methyl ester (75%). ^{1}H NMR ($CDCl_3$, 400 MHz): δ 6.73 (2H, tt, J = 6.8, 2.4 Hz), 6.73 (1H, tt, J = 11.2, 2.4 Hz), 6.22 (1H, brs), 3.67 (3H, s), 3.50 (2H, t, J = 6.0 Hz), 2.53 (2H, t, J = 6.0 Hz). HR-EIMS calcd for $C_{12}H_{13}F_2NO_3$ 258.0941. Found 258.0946. The treatment with NaOH gave **4h** (81%) as amorphous solid. ^{1}H NMR ($CDCl_3$, 400 MHz): δ 7.02 (1H, brs), 6.74 (2H, tt, J = 6.6, 2.4 Hz), 6.63 (1H, tt, J = 11.2, 2.4 Hz), 3.40 (3H, s), 3.73 (2H, t, J = 6.0 Hz), 2.42 (2H, t, J = 6.0 Hz). ^{13}C NMR ($CDCl_3$, 100.6 MHz): δ 172.4, 170.4, 164.1 (d, J = 124.7 Hz), 161.6 (d, J = 124.7 Hz); 138.4 (t, J = 92.6 Hz), 112.1 (d, J = 70.4 Hz), 111.8 (d, J = 70.4 Hz), 102.4 (t, J = 245.8 Hz), 35.1, 33.4. HR-ESIMS calcd for $C_{11}H_{12}F_2NO_3$ 244.0780 ($M + H^+$). Found 244.0785.

4.2.25. (R)-2-[2-(3,5-Difluorophenyl)acetamido]-3-(tritylthio) propanoic acid (**4i**)

L-Cysteine methyl ester hydrochloride (1.00 g, 5.83 mmol) was dissolved in 6 ml of CH_2Cl_2, then trityl chloride (3.57 g, 12.8 mmol) was added and the reaction mixture was stirred at r.t. for 42 h and was quenched with the addition of 0.5 M HCl solution. The not reacted trityl chloride was eliminated with ethyl acetate extraction, then the aqueous layer was basified to pH 9 with saturated solution of $NaHCO_3$ and the product was extracted with AcOEt. The organic layer was washed with water, brine, filtered and concentrated that furnished the desired product. Viscous oil (1.19 g, 60%). ^{1}H NMR ($CDCl_3$, 300 MHz): δ 7.41–7.45 (6H, m), 7.18–7.28 (9H, m), 3.65 (3H, s), 3.20 (1H, dd, J = 7.5, 4.8 Hz), 2.59 (1H, dd, J = 12.6, 4.8 Hz), 2.47 (1H, dd, J = 12.6, 7.5 Hz). HR-FABMS calcd for $C_{30}H_{25}F_2NO_3S$: 400.1347 $[M + Na]^+$. Found 400.1345. S-trityl-L-cysteine methyl ester hydrochloride and 3,5-difluorophenylacetic acid were reacted according the general procedure B. The crude product was directly treated with NaOH to give **4i** (83%) as amorphous solid. ^{1}H NMR ($CDCl_3$, 300 MHz): δ 7.34–7.37 (6H, m), 7.18–7.28 (9H, m), 6.81 (2H, tt, J = 6.6, 2.4 Hz), 6.68 (1H, tt, J = 11.2, 2.4 Hz), 6.58 (1H, d, J = 9.6 Hz), 4.47 (1H, m), 3.69 (2H, s), 2.67 (2H, d, J = 7.6 Hz). HR-FABMS calcd for $C_{30}H_{25}F_2NO_3SNa$ 540.1421 $[M + Na]^+$. Found 540.1422.

4.2.26. (S)-2-[(3,5-Difluorophenyl)acetamido]propanoic acid (**4j**)

From L-alanine methyl ester hydrochloride and 3,5-difluorophenylacetic with the procedure B. Flash chromatography (Ethyl acetate/Hexane = 1/1) gave the methyl ester (82%). ^{1}H NMR ($CDCl_3$, 400 MHz) δ 6.83 (2H, tt(dddd), J = 6.6, 2.4 Hz), 6.73 (1H, tt(dddd), J = 11.2, 2.4 Hz), 6.26 (1H, d, J = 5.2 Hz), 4.58 (1H, qd (dddd), J = 7.2 Hz), 3.74 (3H, s), 3.55 (2H, s), 1.39 (3H, d, J = 7.2 Hz). ^{13}C NMR ($CDCl_3$, 100.6 MHz) δ 173.3, 168.9, 164.3 (d, J_{C-F} = 131.8 Hz), 161.8 (d, J_{C-F} = 131.8 Hz), 138.2 (t(dd), J_{C-F} = 93.1 Hz), 112.3 (d, J_{C-F} = 70.4 Hz), 112.1 (d, J_{C-F} = 70.4 Hz), 102.8 (t(dd), J_{C-F} = 253 Hz), 52.5, 48.2, 42.8, 18.2. The treatment with NaOH gave **4j** (68%) as amorphous solid. ^{1}H NMR ($CDCl_3$, 300 MHz) δ 6.82 (2H, tt(dddd), J = 6.6, 2.1 Hz), 6.75 (1H, tt(dddd), J = 9.3, 2.1 Hz), 6.03 (1H, d, J = 6.0 Hz), 4.60 (1H, qd (dddd), J = 7.2 Hz), 3.57 (2H, s), 1.45 (3H, d, J = 7.2 Hz). ^{13}C NMR (100.6 MHz, CD_3OD) δ 175.9, 172.4, 165.6 (d, J_{C-F} = 49.9 Hz), 163.2 (d, J_{C-F} = 49.5 Hz), 141.0 (t, J_{C-F} = 40.0 Hz), 113.2 (d, J_{C-F} = 28.0 Hz), 113.0 (d, J_{C-F} = 28.0 Hz), 102.9 (t, J_{C-F} = 102.0 Hz), 48.2, 42.7, 17.5.

4.2.27. (R)-2-[(3,5-Difluorophenyl)acetamido]propanoic acid (**4k**)

The application of the procedure described for the preparation of **4j** and the use of D-alanine methyl ester hydrochloride as starting material resulted in the obtainment of **4k**.

4.2.28. (S)-2-[2-(4-Methylphenyl)acetamido]-3-phenylpropanoic acid (**4l**)

From L-phenylalanine methyl ester hydrochloride and *p*-tolylacetic acid with procedure B. Flash chromatography (MeOH:CH_2Cl_2 = 95:5) gave the methyl ester. ^{1}H NMR ($CDCl_3$, 300 MHz) δ 7.18–7.20 (3H, m), 7.13 (2H, d, J = 7.8 Hz), 7.06 (2H, d, J = 7.8 Hz), 6.89 (2H, dd, J = 2.4, 7.2 Hz), 5.78 (1H, d, J = 6.6 Hz), 4.81–4.88 (1H, m), 3.70 (3H, s), 3.51 (2H, s), 3.06 (1H, dd, J = 6.0, 13.6 Hz), 2.98 (1H, dd, J = 6.0, 13.6 Hz), 2.35 (3H, s). The treatment with NaOH gave **4l** (95%) as amorphous solid. ^{1}H NMR ($CDCl_3$, 300 MHz) δ 7.19–7.21 (3H, m), 7.11 (2H, d, J = 7.8 Hz), 7.01 (2H, d, J = 7.8 Hz), 6.94 (2H, dd, J = 2.2, 7.6 Hz), 5.80 (1H, d, J = 6.8 Hz), 4.75–4.82 (1H, m), 3.51 (2H, s), 3.14 (1H, dd, J = 5.4, 14.0 Hz), 3.02 (1H, dd, J = 6.8, 14.0 Hz), 2.35 (3H, s).

4.2.29. General procedures for the preparation of compounds **5**–**8**

Procedure A: A solution of **4** (0.35 mmol), HOBt (0.38 mmol), BOPCl (0.38 mmol) and DIPEA (1.4 mmol) in CH_2Cl_2 was stirred for 10 min at r.t. A solution of amine **3** (0.35 mmol) in CH_2Cl_2 was added and the mixture was stirred for 48 h at r.t. After treatment with $NaHCO_3$ (sat. sol.) the mixture was washed with AcOEt. The organic layers were washed with brine and dried on $MgSO_4$. *Procedure B:* HATU (0.38 mmol) and DIPEA (0.7 mmol) were added to a solution of **4** (0.38 mmol) in THF. The solution was stirred for 15 min at rt. After the addition of **3** (0.35 mmol) the solution was stirred overnight at r.t. *Procedure C:* A solution of **4** (0.35 mmol), DCI (0.35 mmol), HOBt (0.35 mmol) in CH_2Cl_2 was stirred for 15 min. A solution of amine **3** (0.62 mmol) in CH_2Cl_2 was added and the

solution war stirred for 17 h at rt. After treatment with $NaHCO_3$ (sat. sol.) the mixture was washed with AcOEt. The organic layers were washed with brine and dried on $MgSO_4$.

4.2.30. (S)-N-[4-(7-Benzyl-5,6,7,8-tetrahydroimidazo[2′,1′:2,3] thiazolo[5,4-c]pyridin-2-yl)phenyl]-2-[2-(3,5-dimethylphenyl) acetamido]-3-phenylpropanamide (**5a**)

From **3a** and **4a** using general procedure A. Flash chromatography (MeOH:CH_2Cl_2 1:99) to give **5a** (55%) as amorphous solid; $[\alpha]_D^{20} = +3.60$ (c 0.23, MeOH). ^{1}H NMR ($CDCl_3$ with drops of CD_3OD, 400 MHz): δ 9.37 (1H, brs), 7.69 (2H, d, $J = 8.8$ Hz), 7.56 (1H, s), 7.47 (2H, d, $J = 8.4$ Hz), 7.38 (1H, s), 7.37 (1H, d, $J = 1.6$ Hz), 7.32–7.47 (3H, m), 7.20–7.24 (3H, m), 7.10 (2H, dd, $J = 7.2$, 2.4 Hz), 6.91 (1H, s), 6.82 (1H, d, $J = 8.0$ Hz), 6.78 (2H, s), 4.75 (1H, dt, $J = 14.8$, 7.2 Hz), 3.79 (2H, 2H), 3.62 (2H, s), 3.46 (2H, s), 3.09 (1H, dd, $J = 14.0$, 6.8 Hz), 3.02 (2H, t, $J = 5.6$ Hz), 2.98 (1H, dd, $J = 14.0$, 6.8 Hz), 2.80 (2H, t, $J = 5.6$ Hz), 2.28 (6H, s). ^{13}C NMR ($CDCl_3$ with drops of CD_3OD, 100.6 MHz): δ 172.01, 169.29, 148.34, 145.89, 138.21, 136.84, 136.83, 136.66, 135.95, 133.89, 129.91, 129.04, 128.98, 128.75, 128.37, 128.24, 127.50, 126.82, 126.67, 125.34, 124.53, 120.23, 120.14, 118.88, 105.56, 61.01, 54.72, 50.02, 48.48, 42.95, 38.02, 22.53, 20.90 (2C); HR EIMS calcd for $C_{40}H_{40}N_5O_2S$ m/z $[M + H]^+$ 654.2902. Found 654.2889.

4.2.31. (R)-N-[4-(7-Benzyl-5,6,7,8-tetrahydroimidazo[2′,1′:2,3] thiazolo[5,4-c]pyridin-2-yl)phenyl]-2-[2-(3,5-dimethylphenyl) acetamido]-3-phenylpropanamide (**5b**)

From **3a** and **4b** using procedure **A**. Flash chromatography (MeOH:CH_2Cl_2 1:99) to give **5b** (45%) as a white amorphous solid $[\alpha]_D^{20} = -3.40$ (c 0.20, MeOH). ^{1}H NMR ($CDCl_3$ with drops of CD_3OD, 400 MHz): δ 9.37 (1H, brs), 7.69 (2H, d, $J = 8.8$ Hz), 7.56 (1H, s), 7.47 (2H, d, $J = 8.4$ Hz), 7.38 (1H, s), 7.37 (1H, d, $J = 1.6$ Hz), 7.32–7.47 (3H, m), 7.20–7.24 (3H, m), 7.10 (2H, dd, $J = 7.2$, 2.4 Hz), 6.91 (1H, s), 6.82 (1H, d, $J = 8.0$ Hz), 6.78 (2H, s), 4.75 (1H, dt, $J = 14.8$, 7.2 Hz), 3.79 (2H, 2H), 3.62 (2H, s), 3.46 (2H, s), 3.09 (1H, dd, $J = 14.0$, 6.8 Hz), 3.02 (2H, t, $J = 5.6$ Hz), 2.98 (1H, dd, $J = 14.0$, 6.8 Hz), 2.80 (2H, t, $J = 5.6$ Hz), 2.28 (6H, s). ^{13}C NMR ($CDCl_3$ with drops of CD_3OD, 100.6 MHz): δ 172.01, 169.29, 148.34, 145.89, 138.21, 136.84, 136.83, 136.66, 135.95, 133.89, 129.91, 129.04, 128.98, 128.75, 128.37, 128.24, 127.50, 126.82, 126.67, 125.34, 124.53, 120.23, 120.14, 118.88, 105.56, 61.01, 54.72, 50.02, 48.48, 42.95, 38.02, 22.53, 20.90 (2C). HR EIMS calcd for $C_{40}H_{40}N_5O_2S$ m/z $[M + H]^+$ 654.2902. Found 654.2891.

4.2.32. (S)-N-[4-(7-Benzyl-5,6,7,8-tetrahydroimidazo[2′,1′:2,3] thiazolo[5,4-c]pyridin-2-yl)phenyl]-3-[2-(3,5-difluorophenyl) acetamido]propanamide (**5c**)

From **3a** and **4h** using procedure **A**. Flash chromatography (MeOH:CH_2Cl_2 3:97) to give **5c** (70%) as an amorphous solid. ^{1}H NMR ($CDCl_3$ with drops of CD_3OD, 400 MHz): δ 9.48 (1H brs), 7.72 (2H, dt, $J = 9.2$, 1.6 Hz), 7.58 (1H, s), 7.55 (1H, dt, $J = 9.2$, 1.6 Hz), 7.30–7.38 (5H, m), 6.82 (1H, tt, $J = 6.4$, 2.4 Hz), 6.69 (1H, tt, $J = 11.2$, 2.4 Hz), 3.80 (2H, s), 3.64 (2H, s), 3.52 (2H, dd, $J = 12.0$; 6.4 Hz), 3.48 (2H, s), 3.03 (2H, t, $J = 5.6$ Hz), 2.83 (2H, t, $J = 5.6$ Hz), 2.57 (2H, t, $J = 6.4$ Hz). ^{13}C NMR ($CDCl_3$ with drops of CD_3OD, 100.6 MHz): δ 172.96, 170.27, 163.97 (d, $J = 123.7$ Hz), 161.52 (d, $J = 132.8$ Hz), 148.32, 145.90, 138.48 (t, $J = 92.6$ Hz), 137.13, 136.84, 129.61, 128.94, 128.32, 127.45, 124.58, 119.93, 118.92, 111.90 (d, $J = 70.4$ Hz), 111.72 (d, $J = 69.4$ Hz), 105.56, 102.21 (t, $J = 253.0$ Hz), 61.00, 50.00, 48.46, 42.41, 35.96, 33.74, 22.51. HR EIMS calcd for $C_{32}H_{29}F_2N_5O_2S$ m/z $[M + H]^+$ 586.2088. Found 586.2077.

4.2.33. (R)-N-[4-(7-Benzyl-5,6,7,8-tetrahydroimidazo[2′,1′:2,3] thiazolo[5,4-c]pyridin-2-yl)phenyl]-2-[2-(3,5-difluorophenyl) acetamido]-3-sulfanylpropanamide (**5d**)

From **3a** and **4i** using procedure C. Flash chromatography (MeOH:CH_2Cl_2 1:99) to give **5d** (70%) as white solid. ^{1}H NMR ($CDCl_3$, 300 MHz): δ 8.36 (1H, brs), 7.67 (1H, dt, $J = 8.1$, 1.5 Hz), 7.47 (1H, s), 7.15–7.40 (22H, m), 6.87 (1H, brs), 6.73 (2H, dt, $J = 6.4$, 2.4 Hz), 6.66 (tt, $J = 6.4$, 2.4 Hz), 4.24 (1H, tt, $J = 11.2$, 2.4 Hz), 3.75 (2H, s), 3.57 (2H, s), 3.41 (2H, s), 2.97 (2H, t, $J = 5.4$ Hz), 2.73 (2H, t, $J = 5.4$ Hz), 2.67 (2H, d, $J = 6.3$ Hz). S-trityl protected **5d** (0.27 g, 0.29 mmol) was dissolved in anhydrous CH_2Cl_2, then were added TFA (2.3 ml, 2.92 mmol) and Et_3SiH (0.11 g, 0.96 mmol). The reaction was stirred at rt for 1 h. The mixture was concentrated under vacuum and dissolved in AcOEt, washed with $NaHCO_3$ satured solution, water and brine. The crude was filtered, concentrated under vacuum and purified by flash chromatography (AcOEt:Hex 1:1) to afford **5d** as pale yellow amorphous solid (0.08 g, yield 40%). $[\alpha]_D^{20} = +2.30$ (c 0.17, CH_2Cl_2). ^{1}H NMR ($CDCl_3$ with drops of CD_3OD, 400 MHz): δ 9.48 (1H, brs), 7.78 (1H, d, $J = 8.0$ Hz), 7.73 (1H, dt, $J = 9.2$, 1.6 Hz), 7.58 (1H, s), 7.56 (1H, dt, $J = 9.2$, 1.6 Hz), 7.30–7.38 (5H, m), 6.88 (2H, tt, $J = 6.4$, 2.4 Hz), 6.73 (1H, tt, $J = 11.2$, 2.4 Hz), 3.80 (2H, s), 3.66 (2H, s), 3.63 (1H, s), 3.60 (2H, s), 3.37 (1H, qd, $J = 5.6$ Hz), 3.03 (2H, t, $J = 5.6$ Hz), 2.95 (1H, dd, $J = 9.6$, 6.0 Hz), 2.87 (1H, dd, $J = 9.6$, 6.0 Hz), 2.82 (2H, t, $J = 5.6$ Hz,). ^{13}C NMR ($CDCl_3$ with drops of CD_3OD, 100.6 MHz): δ 170.61, 168.12, 164.00 (d, $J = 132.8$ Hz), 161.52 (d, $J = 123.7$ Hz), 148.32, 145.73, 138.18 (t, $J = 98.6$ Hz), 136.74, 136.55, 130.24, 128.93, 128.29, 127.43, 125.33, 124.55, 120.16, 118.91, 112.00 (d, $J = 70.4$ Hz), 111.81 (d, $J = 62.4$ Hz), 105.67, 102.30 (t, $J = 253.0$ Hz), 60.95, 55.39, 49.98, 48.34, 42.03, 26.06, 22.45. HR EIMS calcd for $C_{32}H_{29}F_2N_5O_2S_2$ m/z $[M + H]^+$ 618.1809. Found 618.1792.

4.2.34. (S)-N-[4-(5,6,7,8-Tetrahydroimidazo[2,1-b]benzothiazol-2-yl)phenyl]-2-[2-(3,5-dimethylphenyl)acetamido]-3-phenylpropanamide (**6**)

From **3b** and **4a** using procedure B. Flash chromatography (EtOH:CH_2Cl_2 1:30) to give **6** (91%) as a white solid. mp 225–228 °C, $[\alpha]_D^{20} = +5.79$ (c 0.96, $CHCl_3$). ^{1}H NMR (DMSO-d_6, 400 MHz): δ 10.14 (1H, s), 8.44 (1H, d, $J = 8.2$ Hz), 8.10 (1H, s), 7.77 (2H, d, $J = 8.6$ Hz), 7.60 (2H, d, $J = 8.6$ Hz), 7.31–7.19 (5H, m), 6.81 (1H, s), 6.75 (2H, s), 4.70–4.67 (1H, m), 3.39 (1H, d, $J = 14.1$ Hz), 3.32 (1H, d, $J = 14.1$ Hz), 3.07 (1H, dd, $J = 14.2$, 4.9 Hz), 2.90 (1H, dd, $J = 14.2$, 9.6 Hz), 2.72–2.68 (4H, m), 2.20 (6H, bs), 1.89–1.85 (4H, m). ^{13}C NMR (DMSO-d_6, 100.6 MHz): δ 171.31, 171.13, 148.12, 146.22, 138.74, 138.63, 138.05, 137.11 (2C), 131.12, 131.97, 130.32 (2C), 129.15 (2C), 128.78, 127.88 (2C), 127.45, 126.03 (2C), 121.57, 120.69 (2C), 107.97, 55.97, 43.09, 38.90, 24.91, 23.83, 23.28, 22.30, 21.97(2C). HR EIMS calcd for $C_{34}H_{34}N_4O_2S$ m/z $[M + H]^+$ 562.2402. Found 562.2408.

4.2.35. (S)-N-[4-(Imidazo[2,1-b]benzothiazol-2-yl)phenyl]-2-[2-(3,5-dimethylphenyl)acetamido]-3-phenylpropanamide (**7a**)

From **3c** and **4a** (0.70 g, 2.25 mmol) using procedure B. Flash chromatography (EtOH:CH_2Cl_2 1:30) and crystallization with $CHCl_3$ to give **7a** (75%) as white solid. Mp 224–226 °C, $[\alpha]_D^{20} = +4.52$ (c 1.28, $CHCl_3$). ^{1}H NMR ($CDCl_3$, 400 MHz): δ 8.60 (1H, s), 7.92 (1H, s), 7.79 (2H, d, $J = 8.4$ Hz), 7.70 (1H, d, $J = 7.8$ Hz), 7.61 (1H, d, $J = 7.8$ Hz), 7.48–7.44 (3H, m), 7.37 (1H, t, $J = 7.8$ Hz), 7.29–7.21 (3H, m), 7.12–7.10 (2H, m), 6.95 (1H, s), 6.78 (2H, s), 6.29 (1H, d, $J = 7.6$ Hz), 4.92–4.86 (1H, m), 3.51–3.47 (2H, m), 3.14 (1H, dd, $J = 14.0$, 6.4 Hz), 3.05 (1H, dd, $J = 14.0$, 7.8 Hz), 2.30 (6H, s); ^{13}C NMR ($CDCl_3$, 100.6 MHz): δ 172.60, 170.02, 148.34, 146.43, 139.19, 138.16, 137.08, 134.73 (2C), 132.56, 131.01, 130.79, 129.91 (2C), 129.76, 129.22 (2C), 127.78 (2C), 127.56, 127.16, 126.44 (2C), 125.91, 124.80, 121.00 (2C), 113.68, 107.62, 55.99, 44.11, 38.48, 21.84 (2C). HR EIMS calcd for $C_{34}H_{30}N_4O_2S$ m/z $[M + H]^+$ 558.2089. Found 558.2086.

4.2.36. (R)-N-[4-(Imidazo[2,1-b]benzothiazol-2-yl)phenyl]-2-[2-(3,5-dimethylphenyl)acetamido]-3-phenylpropanamide (**7b**)

From **3c** and **4b** using procedure B. Flash chromatography (EtOH:CH_2Cl_2 1:30) and crystallization with $CHCl_3$ to give **7b** (78%)

as white solid. Mp 224–226 °C, $[\alpha]_D^{20} = -4.28$ (c 0.83, $CHCl_3$). ^1H NMR ($CDCl_3$, 400 MHz): δ 8.60 (1H, s), 7.92 (1H, s), 7.79 (2H, d, $J = 8.4$ Hz), 7.70 (1H, d, $J = 7.8$ Hz), 7.61 (1H, d, $J = 7.8$ Hz), 7.48–7.44 (3H, m), 7.37 (1H, t, $J = 7.8$ Hz), 7.29–7.21 (3H, m), 7.12–7.10 (2H, m), 6.95 (1H, s), 6.78 (2H, s), 6.29 (1H, d, $J = 7.6$ Hz), 4.92–4.86 (1H, m), 3.51–3.47 (2H, m), 3.14 (1H, dd, $J = 14.0$, 6.4 Hz), 3.05 (1H, dd, $J = 14.0$, 7.8 Hz), 2.30 (6H, s); ^{13}C NMR ($CDCl_3$, 100.6 MHz): δ 172.60, 170.02, 148.34, 146.43, 139.19, 138.16, 137.08, 134.73 (2C), 132.56, 131.01, 130.79, 129.91 (2C), 129.76, 129.22 (2C), 127.78 (2C), 127.56, 127.16, 126.44 (2C), 125.91, 124.80, 121.00 (2C), 113.68, 107.62, 55.99, 44.11, 38.48, 21.84 (2C). HR EIMS calcd for $C_{34}H_{30}N_4O_2S$ *m/z* $[M + H]^+$ 558.2089. Found 558.2088.

4.2.37. (S)-N-[4-(Imidazo[2,1-b]benzothiazol-2-yl)phenyl]-2-[2-(3,5-bis(trifluoromethyl)phenyl) acetamido]-3-phenylpropanamide (**7c**)

From **3c** and **4c** using procedure B. Flash chromatography (Hex:AcOEt 1:1) and crystallization with CH_2Cl_2 to afford **7c** (72%) as white solid. Mp 243–245 °C, $[\alpha]_D^{20} = +1.54$ (c 0.31, DMSO). ^1H NMR (DMSO-d_6, 400 MHz): δ 10.25 (1H, s), 8.71–8.69 (2H, m), 8.04 (1H, d, $J = 8.0$ Hz), 7.98 (1H, d, $J = 8.0$ Hz), 7.96 (1H, s), 7.90 (2H, s), 7.82 (2H, d, $J = 8.6$ Hz), 7.66 (2H, d, $J = 8.6$ Hz), 7.58 (1H, t, $J = 8.0$ Hz), 7.44 (1H, t, $J = 8.0$ Hz), 7.29–7.13 (5H, m), 4.75–4.70 (1H, m), 3.74 (1H, d, $J = 15.1$ Hz), 3.70 (1H, d, $J = 15.1$ Hz), 3.10 (1H, dd, $J = 13.8$, 4.8 Hz), 2.89 (1H, dd, $J = 13.8$, 9.7 Hz). ^{13}C NMR (DMSO-d_6, 100.6 MHz): δ 172.13, 169.45, 146.82, 145.91, 141.12, 139.44, 138.87, 133.21, 131.98 (2C, q, $J = 33.2$ Hz) 131.80, 131.01 (2C), 130.51, 130.23 (2C), 129.03 (2C), 127.79, 127.41, 126.23 (2C), 126.18, 126.10, 123.42 (2C, q, $J = 271.0$ Hz), 121.79, 120.84 (2C), 114.37, 109.56, 56.04, 42.60, 38.65. HR EIMS calcd for $C_{34}H_{24}F_6N_4O_2S$ *m/z* $[M + H]^+$ 666.1524. Found 666.1526.

4.2.38. (R)-N-[4-(Imidazo[2,1-b]benzothiazol-2-yl)phenyl]-2-[2-(3,5-bis(trifluoromethyl)phenyl) acetamido]-3-phenylpropanamide (**7d**)

From **3c** and **4d** using procedure B. Flash chromatography (Hex:AcOEt 1:1) and crystallization with CH_2Cl_2 to afford **7d** (74%) as white solid. Mp 243–245 °C, $[\alpha]_D^{20} = -1.46$ (c 0.34, DMSO). ^1H NMR (DMSO-d_6, 400 MHz): δ 10.25 (1H, s), 8.71–8.69 (2H, m), 8.04 (1H, d, $J = 8.0$ Hz), 7.98 (1H, d, $J = 8.0$ Hz), 7.96 (1H, s), 7.90 (2H, s), 7.82 (2H, d, $J = 8.6$ Hz), 7.66 (2H, d, $J = 8.6$ Hz), 7.58 (1H, t, $J = 8.0$ Hz), 7.44 (1H, t, $J = 8.0$ Hz), 7.29–7.13 (5H, m), 4.75–4.70 (1H, m), 3.74 (1H, d, $J = 15.1$ Hz), 3.70 (1H, d, $J = 15.1$ Hz), 3.10 (1H, dd, $J = 13.8$, 4.8 Hz), 2.89 (1H, dd, $J = 13.8$, 9.7 Hz). ^{13}C NMR (DMSO-d_6, 100.6 MHz): δ 172.13, 169.45, 146.82, 145.91, 141.12, 139.44, 138.87, 133.21, 131.98 (2C, q, $J = 33.2$ Hz) 131.80, 131.01 (2C), 130.51, 130.23 (2C), 129.03 (2C), 127.79, 127.41, 126.23 (2C), 126.18, 126.10, 123.42 (2C, q, $J = 271.0$ Hz), 121.79, 120.84 (2C), 114.37, 109.56, 56.04, 42.60, 38.65. HR EIMS calcd for $C_{34}H_{24}F_6N_4O_2S$ *m/z* $[M + H]^+$ 666.1524. Found 666.1528.

4.2.39. (S)-N-[4-(Imidazo[2,1-b]benzothiazol-2-yl)phenyl]-2-[2-(3,5-difluorophenyl)acetamido]-3-phenylpropanamide (**7e**)

From **3c** and **4e** using procedure B. Flash chromatography (Hex:AcOEt 1:1) and crystallization with isopropanol to afford **7e** (62%) as white solid. Mp 242–243 °C, $[\alpha]_D^{20} = -4.34$ (c 0.27, CH_3OH:$CHCl_3$ = 1:1). ^1H NMR (DMSO-d_6, 400 MHz): δ 10.29 (1H, s), 8.73 (1H, s), 8.62 (1H, d, $J = 8.3$ Hz), 8.05 (1H, d, $J = 7.9$ Hz), 7.99 (1H, d, $J = 7.9$ Hz), 7.83 (2H, d, $J = 8.6$ Hz), 7.67 (2H, d, $J = 8.6$ Hz), 7.59 (1H, t, $J = 8.0$ Hz), 7.45 (1H, t, $J = 8.0$ Hz), 7.32–7.20 (5H, m), 7.05 (1H, tt, $J = 9.5$, 2.3 Hz), 6.86 (2H, dd, $J = 8.4$, 2.3 Hz), 4.75–4.70 (1H, m), 3.53 (1H, d, $J = 14.1$ Hz), 3.49 (1H, d, $J = 14.1$ Hz), 3.11 (1H, dd, $J = 13.7$, 4.8 Hz) 2.90 (1H, dd, $J = 13.7$, 9.8 Hz). ^{13}C NMR (DMSO-d_6, 100.6 MHz): δ 170.56, 169.51, 162.53 (2C, dd, $J = 244.5$, 14.1 Hz), 147.29, 146.32, 141.07 (t, $J = 10.1$ Hz), 138.46, 137.94, 132.27, 129.67 (2C), 129.40, 129.32, 128.48 (2C), 127.21, 126.87, 125.61 (2C), 125.57, 125.52, 120.10 (2C), 113.80, 112.62 (2C, d, $J = 24.1$ Hz), 109.01, 102.28 (t, $J = 26.2$ Hz), 55.39, 41.90, 38.31. HR EIMS calcd for $C_{32}H_{24}F_2N_4O_2S$ *m/z* $[M + H]^+$ 566.1588. Found 566.1584.

4.2.40. N-[4-(Imidazo[2,1-b]benzothiazol-2-yl)phenyl]-2-[2-(3,5-dimethylphenyl)acetamido] acetamide (**7f**)

From **3c** and **4f** using procedure B. Flash chromatography ($MeOH/CH_2Cl_2$ 1:30) and crystallization with CH_3CN to afford **7f** (72%) as white solid. Mp 250–252 °C ^1H NMR (DMSO-d_6, 400 MHz): δ 10.04 (1H, s), 8.71 (1H, s), 8.37–8.33 (1H, m), 8.05 (1H, d, $J = 7.9$ Hz), 7.98 (1H, d, $J = 7.9$ Hz), 7.82 (2H, d, $J = 8.6$ Hz), 7.66 (2H, d, $J = 8.6$ Hz), 7.59 (1H, t, $J = 7.9$ Hz), 7.44 (1H, t, $J = 7.9$ Hz), 6.92 (2H, s), 6.87 (1H, s), 3.92 (2H, d, $J = 5.6$ Hz), 3.34 (2H, s), 2.26 (6H, s). ^{13}C NMR (DMSO-d_6, 100.6 MHz): δ 171.83, 168.80, 147.93, 147.42, 139.14, 138.16 (2C), 137.09, 132.99, 130.29, 130.21, 128.88, 128.02 (2C), 127.78, 126.29 (2C), 126.17, 126.08, 120.53 (2C), 114.36, 109.48, 44.10, 43.19, 21.99 (2C). EIMS 468 $[M]^+$.

4.2.41. (S)-N-[4-(Imidazo[2,1-b]benzothiazol-2-yl)phenyl]-2-[2-(3,5-dimethylphenyl)acetamido]-3-(4-hydroxyphenyl)propanamide (**7g**)

From **3c** and **4g** using procedure B. Flash chromatography (*i*-PrOH/CH_2Cl_2 95:5) to afford **7g** (52%) as pale yellow solid. Mp 265–268 °C, $[\alpha]_D^{20} = +2.76$ (c 0.26, DMSO). ^1H NMR (DMSO-d_6, 400 MHz): δ 10.25 (1H, s), 8.73 (1H, s), 8.39 (1H, d, $J = 7.8$ Hz), 8.08 (1H, d, $J = 8.1$ Hz), 7.98 (1H, d, $J = 8.1$ Hz), 7.81 (2H, d, $J = 8.6$ Hz), 7.67 (2H, d, $J = 8.6$ Hz), 7.58 (1H, t, $J = 8.1$ Hz), 7.43 (1H, t, $J = 8.1$ Hz), 7.11 (2H, d, $J = 7.5$ Hz), 6.84 (1H, s), 6.78 (2H, s), 6.67 (2H, d, $J = 7.5$ Hz),5.89 (1H, s), 4.65–4.54 (1H, m), 3.48–3.30 (2H, m), 2.98 (1H, dd, $J = 14.2$, 4.5 Hz), 2.81 (1H, dd, $J = 14.2$, 9.3 Hz), 2.53 (6H, s). ^{13}C NMR (DMSO-d_6, 100.6 MHz): δ 171.64, 169.12, 154.75, 147.78, 146.05, 138.85, 138.06, 134.65 (2C), 132.84 (2C), 132.24, 130.77, 130.61, 130.19, 129.12, 127.13 (2C), 116.78 (2C), 127.02, 126.08 (2C), 125.34, 124.63, 120.53 (2C), 112.89, 107.41, 54.11, 44.01, 35.21, 21.81 (2C). EIMS *m/z* $[M]^+$ 574.

4.2.42. (S)-N-[4-(Imidazo[2,1-b]benzothiazol-2-yl)phenyl]-2-[2-(4-methylphenyl)acetamido)-3-phenylpropanamide (**7h**)

From **3c** and **4l** using procedure B. Flash chromatography (CH_2Cl_2/MeOH 5%) to afford **7h** (57%). ^1H NMR ($CDCl_3$ with drops of CD_3OD-d_4, 500 MHz) δ 7.89 (s, 1H-Ar), 7.68 (d, $J = 8.0$ Hz, 2H-Ar), 7.65 (d, $J = 8.0$ Hz, 1H-Ar), 7.57 (d, $J = 8.0$ Hz, 1H-Ar), 7.39–7.43 (m, 3H-Ar), 7.29 (dd, $J = 7.5$, 7.5 Hz, 1H-Ar), 7.16–7.17 (m, 3H-Ar), 7.04–7.06 (m, 4H-Ar), 6.98 (d, $J = 7.5$ Hz, 2H-Ar), 4.70 (dd, $J = 7.5$, 7.5 Hz, 1H, C*H*CH_2Ph), 3.43 (s, 2H, C*H*$_2$CO), 3.05 (dd, $J = 14.0$, 7.5 Hz, 1H, CHC*H*$_2$Ph), 2.92 (dd, $J = 14.0$, 7.5 Hz, 1H, CHC*H*$_2$Ph), 2.27 (s, 3H, CH_3). ^{13}C NMR ($CDCl_3$ with drops of CD_3OD-d_4, 125.7 MHz) δ 172.0, 169.4, 148.0, 146.7, 136.9, 136.7, 135.9, 131.9, 131.0, 129.8, 129.5, 129.4, 129.1, 128.9, 128.3, 126.7, 126.3, 125.5, 124.9, 124.2, 120.2, 112.6, 106.7, 54.7, 42.6, 38.1, 20.8. EIMS *m/z* $[M + H]+$ 545.2.

4.2.43. (S)-N-[4-(Imidazo[2,1-b]benzothiazol-2-yl)phenyl]-2-[2-(3,5-dimethylphenyl)acetamido]-3-(4-methylphenyl)propanamide (**7i**)

HATU (258 mg, 0.68 mmol) and DIPEA (197 μl, 1.13 mmol) were added to a solution of **3c** (150 mg, 0.56 mmol) and (*S*)-*N*-Boc-4-methylphenylalanine (158 mg, 0.56 mmol) in dry THF (11 ml). After 48 h at r.t. the solvent was removed under reduced pressure and the crude mixture was purified by flash chromatography (CH_2Cl_2:MeOH 1%) to afford the intermediate that was directly used for the next step. ESIMS *m/z* $[M + H]^+$ 527.2. The obtained compound was dissolved in dry CH_2Cl_2 (5 ml). TFA (5 ml) was then added and the reaction mixture was stirred at r.t. for 4 h. Then the solvent was removed under reduced pressure and the crude mixture was purified by flash chromatography (CH_2Cl_2:EtOH 10%) to afford the corresponding free amine (227 mg, 95%).

^{1}H NMR (CD_3OD-d_4, 400 MHz) δ 8.31 (1H, s), 7.79 (2H, dd, J = 8.0, 8.0 Hz), 7.73 (2H, d, J = 6.8 Hz), 7.54 (2H, d, J = 6.8 Hz), 7.47 (1H, dd, J = 8.0, 8.0 Hz), 7.35 (1H, dd, J = 8.0, 8.0 Hz), 7.16 (2H, dd, J = 16.2, 7.8 Hz), 4.20 (1H, dd, J = 7.4, 7.4 Hz), 3.34 (2H, s, 2H), 3.24 (1H, dd, J = 14.0, 7.4 Hz), 3.11 (1H, dd, J = 14.0, 7.4 Hz), 2.28 (3H, s). Anal. Calcd. for $C_{25}H_{22}N_4OS$: C, 70.40; H, 5.2; N, 13.14. Found: C, 70.77; H, 5.18; N, 13.09. 3,5-Dimethylphenylacetic acid (60.6 mg, 0.37 mmol) and DMAP (21.5 mg, 0.17 mmol) were added to a suspension of the previously obtained free amine (150 mg, 0.35 mmol) in dry CH_2Cl_2 (4 ml). Once the product was solved, DCI (83 μl, 0.53 mmol) was added. After 4.5 h at r.t. the solvent was removed under reduced pressure and the crude mixture was purified by flash chromatography (CH_2Cl_2:EtOH 2%) to afford **7i** contaminated with DCI. The product was finally purified by crystallization in $CHCl_3$ (65 mg, 32%). ^{1}H NMR ($CDCl_3$, 400 MHz) δ 8.36 (1H, s), 7.87 (1H, s), 7.74–7.77 (2H, m), 7.63 (2H, d, J = 7.6 Hz), 7.56 (1H, d, J = 7.6 Hz), 7.41–7.45 (3H, m), 7.32 (1H, dd, J = 7.6, 7.6 Hz), 7.05 (2H, d, J = 7.6 Hz), 6.98 (2H, d, J = 7.6 Hz), 6.92 (1H, s), 6.75 (2H, s), 6.14 (1H, d, J = 7.5 Hz), 4.77 (1H, dd, J = 14.4, 7.6 Hz), 3.49 (2H, s), 3.02–3.08 (2H, m), 2.32 (3H, s), 2.27 (6H, s). ^{13}C NMR ($CDCl_3$, 100.4 MHz) δ 172.1, 169.0, 148.0, 147.2, 138.7, 136.9, 136.5 (2C), 133.8, 133.1, 132.1 (2C), 130.2, 130.0, 129.4, 129.2, 129.1 (2C), 127.1, 126.2 (2C), 125.7 (2C), 124.8, 124.3, 120.2 (2C), 112.6, 106.5, 55.3, 43.4, 36.7, 29.7, 21.2, 21.1. ESIMS m/z $[M + H]^+$ 573.2.

4.2.44. (S)-N-[4-(Imidazo[2,1-b]benzothiazol-2-yl)phenyl]-2-[2-(3,5-bis(trifluoromethyl)phenyl)acetamido]-3-(4-methylphenyl) propanamide (**7j**)

3,5-Bis(trifluoromethyl)phenylacetic acid (111 mg, 0.40 mmol) and DMAP (24 mg, 0.19 mmol) were added to a suspension of the free amine used for the preparation of compound **7i** (164 mg, 0.38 mmol) in dry CH_2Cl_2 (4 ml). Once the product was solved, DCI (90 μl, 0.57 mmol) was added. After 4.5 h at r.t. the solvent was removed under reduced pressure and the crude mixture was purified by flash chromatography (CH_2Cl_2:EtOH 2%) to afford **7j** contaminated with DCI. The product was finally purified by crystallization in $CHCl_3$ (115 mg, 44%). ^{1}H NMR ($CDCl_3$, 400 MHz) δ 7.92 (1H, s), 7.73–7.75 (3H, m), 7.68–7.70 (3H, m), 7.61 (1H, d, J = 7.2 Hz), 7.48 (1H, s), 7.46 (1H, s), 7.42 (1H, d, J = 8.2 Hz), 7.33 (1H, dd, J = 8.2, 8.2 Hz), 6.99 (4H, s), 4.68 (1H, dd, J = 7.2, 7.2 Hz), 3.58 (2H, s), 3.06 (1H, dd, J = 14.0, 7.5 Hz), 2.94 (1H, dd, J = 14.0, 7.2 Hz), 2.23 (3H, s). ^{13}C NMR ($CDCl_3$ with drops of CD_3OD-d_4, 125.5 MHz) δ 169.7, 166.0, 147.7, 145.3, 137.4 (2C), 137.2 (2C), 136.5 (2C), 132.7, 131.7 (2C), 131.4, 129.9, 129.3, 129.4, 129.1 (2C), 128.9, 126.6 (2C), 125.7 (2C), 125.5, 124.4, 120.9, 120.4 (2C), 113.0, 107.0, 55.0, 42.0, 37.9, 20.6. ESIMS m/z $[M + H]^+$ 681.2.

4.2.45. (S)-N-[4-(7-Bromoimidazo[2,1-b]benzothiazol-2-yl) phenyl]-2-[2-(3,5-bis(trifluoromethyl) phenyl)acetamido]-3-phenylpropanamide (**7k**)

From **3e** and **4c** using procedure B. Flash chromatography (Hex:AcOEt = 1:1) to afford **7k** (48%) as a white solid. $[\alpha]_D^{20}$ = 2.95 (Na, c = 0.28 in DMSO). ^{1}H NMR (DMSO-d_6, 400 MHz): δ 10.26 (1H, s), 8.71 (1H, d, J = 8.7 Hz), 8.70 (1H, s), 8.34 (1H, d, J = 1.8 Hz), 7.95 (1H, s), 7.93 (1H, d, J = 8.5 Hz), 7.89 (2H, s), 7.81 (2H, d, J = 8.7 Hz), 7.75 (1H, dd, J = 8.5, 1.8 Hz), 7.66 (2H, d, J = 8.7 Hz), 7.27–7.13 (5H, m), 4.75–4.69 (1H, m), 3.75 (1H, d, J = 16.4 Hz), 3.70 (1H, d, J = 16.4 Hz), 3.10 (1H, dd, J = 13.8, 4.8 Hz), 2.89 (1H, dd, J = 13.8, 9.8 Hz). ^{13}C NMR (DMSO-d_6, 100.6 MHz): δ 170.48, 169.49, 147.42, 146.85, 140.10, 138.44, 137.86, 131.82, 131.59, 130.58 (2C, q, J = 37 Hz), 130.37 (2C), 129.99, 129.59, 129.50, 128.40 (2C), 127.86, 126.80 (2C), 125.60 (2C), 123.85 (2C, q, J = 272 Hz), 120.68, 120.11, 117.12, 115.29, 109.14, 55.42, 41.48, 38.30. HR-EIMS Calcd for $[C_{34}H_{23}BrF_6N_4O_2S]^+$ 744.0629; Found 744.06134.

4.2.46. (S)-N-[4-(6-Benzyl-5,6,7,8-tetrahydroimidazo[2′,1′:2,3] thiazolo[4,5-c]pyridin-2-yl)phenyl]-3-[2-(3,5-difluorophenyl) acetamido]propanamide (**8a**)

From **3d** and **4h** using procedure B. Flash chromatography (CH_2Cl_2/MeOH = 99/1) to give **8a** (65%). ^{1}H NMR ($CDCl_3$ with drops of CD_3OD, 400 MHz) δ 9.40 (1H, bs), 7.67 (1H, dt(ddd), J = 8.8, 1.6, 1.6 Hz), 7.52 (1H, dt(ddd), J = 8.8, 1.6, 1.6 Hz), 7.47 (1H, t(dd), J = 5.6 Hz), 7.43 (1H, s), 7.30–7.41 (6H, m), 6.80 (2H, tt(dddd), J = 6.4, 2.4 Hz), 6.67 (1H, tt(dddd), J = 11.2, 2.4 Hz), 3.81 (2H, s), 3.59 (2H, s), 3.51 (2H, dt, J = 12.4; 6.4 Hz), 3.47 (2H, s), 2.96 (2H, t(dd), J = 5.2 Hz), 2.83 (2H, t(dd), J = 5.2 Hz), 2.55 (2H, t(dd), J = 6.0 Hz). ^{13}C NMR ($CDCl_3$ with drops of CD_3OD-d_4, 100.6 MHz) δ 170.84 (d, J = 90.5 Hz), 170.27 (d, J = 93.6 Hz), 164.05 (d, J_{C-F} = 123.7 Hz), 161.57 (d, J_{C-F} = 132.8 Hz), 145.92, 148.68, 138.47 (t(dd), J_{C-F} = 93.6 Hz), 137.12 (t(dd), J_{C-F} = 92.6 Hz), 137.11, 136.98, 129.69, 128.89, 128.44, 127.52, 125.36, 124.11, 119.95, 119.89, 112.01(d, J_{C-F} = 69.4 Hz), 111.83 (d, J_{C-F} = 70.4 Hz), 105.28, 102.35 (t(dd), J_{C-F} = 253.0 Hz), 61.55, 50.04, 48.94, 42.61, 36.06, 35.92, 24.47. HRMS calculated for $C_{32}H_{30}F_2N_5O_2S$ $[M + H]^+$: 586.2088; Found: 586.2075.

4.2.47. (S)-N-[4-(6-Benzyl-5,6,7,8-tetrahydroimidazo[2′,1′:2,3] thiazolo[4,5-c]pyridin-2-yl)phenyl]-2-[2-(3,5-difluorophenyl) acetamido]propanamide (**8b**)

From **3d** and **4j** using procedure B. Flash chromatography (CH_2Cl_2/MeOH = 99/1) to give **8b** (48%). $[\alpha]_D^{20}$ = +3.8 (c 0.17, MeOH); ^{1}H NMR ($CDCl_3$ with drops of CD_3OD, 400 MHz) δ 9.54 (brs, 1H, NH), 7.67 (dt(ddd), J = 8.8, 1.6, 1.6 Hz, 1H, CH_{Ar}), 7.63 (d, J = 7.6 Hz, 1H, NH), 7.52 (dt(ddd), J = 8.8, 1.6, 1.6 Hz, 1H, CH_{Ar}), 7.32–7.42 (m, 6H, 5CH_{Ar}, H-3), 6.84 (tt(dddd), J = 6.4, 2.4 Hz, 2H, CH_{Ar}), 6.70 (tt(dddd), J = 11.2, 2.4 Hz, 1H, CH_{Ar}), 4.57 (qd, J = 7.2 Hz, 1H, CH), 3.81 (s, 2H, CH_2Ph), 3.58 (s, 2H, H-8), 3.54 (s, 2H, CH_2), 2.95 (t(dd), J = 5.6 Hz, 2H, H-6), 2.82 (t(dd), J = 5.6 Hz, 2H, H-5), 1.41 (d, J = 6.8 Hz, 3H, CH_3). ^{13}C NMR ($CDCl_3$ with drops of CD_3OD-d_4, 100.6 MHz) δ 170.80 (d, J = 101.6 Hz), 170.24 (d, J = 70.4 Hz), 164.05 (d, J_{C-F} = 132.8 Hz), 161.58 (d, J_{C-F} = 124.7 Hz), 145.84, 148.67, 138.30 (t(dd), J_{C-F} = 93.1 Hz), 136.97, 136.90 (t(dd), J_{C-F} = 93.1 Hz), 129.90, 128.87, 128.42, 127.51, 125.38, 124.09, 120.14, 120.05, 119.89, 112.07 (d, J_{C-F} = 69.4 Hz), 111.89 (d, J_{C-F} = 69.4 Hz), 105.32, 102.40 (t(dd), J_{C-F} = 253 Hz), 61.53, 50.02, 49.46, 48.93, 42.25, 24.45, 17.95. HRMS calcd. for $C_{32}H_{30}F_2N_5O_2S$ $[M + H]^+$: 586.2088; Found: 586.2075.

4.2.48. (R)-N-[4-(6-Benzyl-5,6,7,8-tetrahydroimidazo[2′,1′:2,3] thiazolo[4,5-c]pyridin-2-yl)phenyl]-2-[2-(3,5-difluorophenyl) acetamido]propanamide (**8c**)

From **3d** and **4k** using procedure B. Flash chromatography (CH_2Cl_2/MeOH = 99/1) to give **8c** (48%). $[\alpha]_D^{20}$ = −3.6 (c 0.23, MeOH); ^{1}H NMR and ^{13}C NMR see **8b**. HRMS calcd. for $C_{32}H_{30}F_2N_5O_2S$ $[M + H]^+$: 586.2088; Found: 586.2077.

4.3. Biology

4.3.1. Cell culture

MDCK cells were grown in Dulbecco's modified Eagle's medium (DMEM) (Gibco BRL) containing 4 mM L-glutamine and supplemented with 2% (v/v) fetal bovine serum (Gibco BRL), 100 U/ml penicillin, and 100 μg/ml streptomycin. Cells were plated at a density of 1000 cells per well in 24-well microplates and allowed settling overnight at 37 °C in a humidified atmosphere of 5% CO_2 prior to treatments. Human MCF10A breast cells, human MDA-MB231 breast cancer cells, human GTL-16 gastric carcinoma cells, human HepG2 hepatocellular carcinoma, and human BT474 breast cancer cells were grown in RPMI medium (Gibco BRL) containing 4 mM L-glutamine and supplemented with 10% (v/v) fetal bovine

serum (Gibco BRL), 100 U/ml penicillin, and 100 μg/ml streptomycin and kept at 37 °C in a humidified atmosphere of 5% CO_2.

4.3.2. Primary cultures of embryonic cortical neurons and hepatocyte

Primary embryonic cortical and hepatocyte cultures and survival assays were performed as previously described [11,12,49]. For toxicity assays, primary cells were exposed to compound **7c** for 24 h. Viability was assessed with the Cell Titer Glo Luminescent Assay (Promega), according to the manufacturer's instructions. Data on biological assays were performed in quadruplicate.

4.3.3. Compound treatments

For scattering assays, MDCK cells were pre-incubated with compounds overnight at 0.1–100 μM concentrations at 37 °C in a humidified atmosphere of 5% CO_2, followed by a 24 h stimulation with 20 ng/ml HGF (R&D Systems), as previously described [32]. Cells were further incubated at 37 °C in an atmosphere of 5% CO_2 for 24–48 h, washed with phosphate-buffered saline (PBS; Gibco BRL), and fixed with 4% PFA (Sigma). The quantification of scattering response was performed by counting the number of cells with scattered morphology in 30 independent colonies. The IC_{50} corresponds to the concentration of compounds leading to a 50% inhibition of Met-triggered cell scattering. Active compounds were assayed to impair scattering response also on MCF10A cells following the same procedure. For survival assays, cells were cultured in serum-free media for 24 h prior to compound addition for 48 h. Viability was assessed with the Cell Titer Glo Luminescent Assay (Promega). For in vitro tumorigenesis, soft agar growth assays were performed using GTL-16 and HepG2 cells, as previously described [32]. Data on biological assays are representative of three independent experiments performed in duplicate. For the Ba/F3 cell assay, a total of 2.10^4 cells/well/50 μl were seeded in a 96-wells plate. Treatment was initiated by addition of a 2× drug solution of ½ serial dilutions ranging from 0 to 10 μM. Cells were grown for 48 h at 37 °C and then incubated with 10 μl/well of Cell Titer Blue (G8080; Promega). Proliferation was quantified by measuring the absorbance at 490 nm using a scanning multiwell spectrophotometer (MultiSkan MS, Thermo-LabSystems, France). A blank well without cells was used as a background control for the spectrophotometer and all assays were performed in triplicate.

4.3.4. Biochemical evaluation of Met inhibitors

After starvation, cells were pretreated overnight with inhibitors, then stimulated with HGF (20 ng/ml), and total extracts were analyzed as described [10]. Antibodies used were anti-tubulin (Sigma), anti-phospho Tyr1234/1235-Met, anti phospho-ErbBs, anti-ERKs (Cell Signaling), anti-ErbBs, anti-Met (Santa Cruz).

4.3.5. Protein kinase assay

The inhibitory profile of 7c toward Met RTK was performed by applying the Kinexus compound profiling service.

4.3.6. In vivo tumorigenesis assays

Xenografts of GTL-16 cells were established by intraperitoneal (i.p.) injection of cells (10^6) in nude mice (S/SOPF SWISS NU/NU; Charles River). Mice were treated with **7c** (i.p. 10 or 30 mg kg^{-1}) or vehicle at day 1 and treatment was repeated every other day. Mice were then sacrificed after 21 days of treatment. Tumor nodules present in the peritoneal cavity were isolated and quantified according to their total weight. For **7c** in vivo treatment, the drug was formulated in Cremophor EL-DMSO (1:1, v/v) and diluted in sterile 0.9% (w/v) sodium chloride for administration at dose levels of 10 and 30 mg kg^{-1}. Two independent tumorigenesis assays were performed (8 mice per group were used). Mice were kept at the IBDML animal facilities. All experimental procedures were performed according to the European Union and institutional guidelines for the care and use of laboratory animals, and were approved by an official committee.

4.3.7. Statistical analysis

Results were expressed as the mean ± s.e.m. Quantification of biological assays and tumor growth in mice was analyzed by the student-*t* test. Statistical significance was defined as ns: $P > 0.05$; *: $P < 0.05$; **: $P < 0.01$; ***: $P < 0.001$. Statistic analysis was carried out using the Analyze-it software for Microsoft Excel (Analyse-it Software, Ltd).

Conflict of interest

The authors declare no conflict of interest.

Acknowledgments

We are particularly grateful to: Patrick Faure, Romain Rauly, Keith Dudley, Sandro De Falco, Fabienne Lamballe, Filippo Conti, and all members of our labs for helpful discussions and comments; Annalisa Fico for her help with in vivo studies and valuable inputs. We thank: Sylvie Richelme for technical contribution; staff at the IBDML animal house facility and technical support; the imaging platform at the IBDML. This work was supported by funds from the INCa (Insitut National du Cancer), ARC (Association pour la recherche contre le cancer), FRM (Fondation pour la recherche médicale), FdF (Fondation de France), Fondation Bettencourt-Schueller, Marie Curie Host Fellowship for the Transfer of Knowledge (MTKD-CT-2004-509804), Protisvalor, Valorpaca, and Oséo to F.M; by the Ministero dell'Istruzione, dell'Università e della Ricerca (MIUR) PRIN 2007 – Program "Sviluppo e caratterizzazione di nuovi inibitori di tirosine chinasi cellulari con attività antiproliferativa e antiangiogenica nei confronti di differenti tumori" to D.P.; and by the Spanish Ministry of Science and Innovation (Project CTQ2009-07021/BQU) and the AGAUR, Generalitat de Catalunya (Grant 2009-SGR-111) to M.A. and J.B. This research has been developed under the umbrella of CM0602 COST Action "Inhibitors of Angiogenesis: design, synthesis and biological exploitation". A.F. was supported by the INCa and ARC; N.I. by Valorpaca.

Appendix. Supplementary information

Supplementary data related to this article can be found online at doi:10.1016/j.ejmech.2011.10.051.

References

[1] E. Zwick, J. Bange, A. Ullrich, Receptor tyrosine kinases as targets for anticancer drugs, Trends Mol. Med. 8 (2002) 17–23.
[2] M.A. Lemmon, J. Schlessinger, Cell signaling by receptor tyrosine kinases, Cell 141 (2010) 1117–1134.
[3] T. Hunter, Tyrosine phosphorylation: thirty years and counting, Curr. Opin. Cell Biol. 21 (2009) 140–146.
[4] B.S. Knudsen, G. Vande Woude, Showering c-MET-dependent cancers with drugs, Curr. Opin. Genet. Dev. 18 (2008) 87–96.
[5] P. Kaposi-Novak, J.S. Lee, L. Gomez-Quiroz, C. Coulouarn, V.M. Factor, S.S. Thorgeirsson, Met-regulated expression signature defines a subset of human hepatocellular carcinomas with poor prognosis and aggressive phenotype, J. Clin. Invest. 116 (2006) 1582–1595.
[6] L. Trusolino, A. Bertotti, P.M. Comoglio, MET signalling: principles and functions in development, organ regeneration and cancer, Nat. Rev. Mol. Cell Biol. 11 (2010) 834–848.
[7] F. Maina, F. Casagranda, E. Audero, A. Simeone, P. Comoglio, R. Klein, C. Ponzetto, Uncoupling of Grb2 from the Met receptor in vivo reveals complex roles in muscle development, Cell 87 (1996) 531–542.
[8] F. Maina, M.C. Hilton, R. Andres, S. Wyatt, R. Klein, A.M. Davies, Multiple roles for hepatocyte growth factor in sympathetic neuron development, Neuron 20 (1998) 835–846.

[9] F. Maina, M.C. Hilton, C. Ponzetto, A.M. Davies, R. Klein, Met receptor signaling is required for sensory nerve development and HGF promotes axonal growth and survival of sensory neurons, Genes Dev. 11 (1997) 3341–3350.
[10] F. Maina, G. Pante, F. Helmbacher, R. Andres, A. Porthin, A.M. Davies, C. Ponzetto, R. Klein, Coupling Met to specific pathways results in distinct developmental outcomes, Mol. Cell 7 (2001) 1293–1306.
[11] A. Moumen, A. Ieraci, S. Patane, C. Sole, J.X. Comella, R. Dono, F. Maina, Met signals hepatocyte survival by preventing Fas-triggered FLIP degradation in a PI3k-Akt-dependent manner, Hepatology 45 (2007) 1210–1217.
[12] A. Moumen, S. Patane, A. Porras, R. Dono, F. Maina, Met acts on Mdm2 via mTOR to signal cell survival during development, Development 134 (2007) 1443–1451.
[13] M. Genestine, E. Caricati, A. Fico, S. Richelme, H. Hassani, C. Sunyach, F. Lamballe, G.C. Panzica, B. Pettmann, F. Helmbacher, C. Raoul, F. Maina, R. Dono, Enhanced neuronal Met signalling levels in ALS mice delay disease onset, Cell Death Dis. 2 (2011) e130.
[14] L. Tonges, T. Ostendorf, F. Lamballe, M. Genestine, R. Dono, J.C. Koch, M. Bahr, F. Maina, P. Lingor, Hepatocyte growth factor protects retinal ganglion cells by increasing neuronal survival and axonal regeneration in vitro and in vivo, J. Neurochem. 117 (2011) 892–903.
[15] A. Furlan, V. Stagni, A. Hussain, S. Richelme, F. Conti, A. Prodosmo, A. Destro, M. Roncalli, D. Barila, F. Maina, Abl interconnects oncogenic Met and p53 core pathways in cancer cells, Cell Death Differ. 18 (2011) 1608–1616.
[16] C.L. Arteaga, HER3 and mutant EGFR meet MET, Nat. Med. 13 (2007) 675–677.
[17] J.M. Stommel, A.C. Kimmelman, H. Ying, R. Nabioullin, A.H. Ponugoti, R. Wiedemeyer, A.H. Stegh, J.E. Bradner, K.L. Ligon, C. Brennan, L. Chin, R.A. DePinho, Coactivation of receptor tyrosine kinases affects the response of tumor cells to targeted therapies, Science 318 (2007) 287–290.
[18] J.A. Engelman, K. Zejnullahu, T. Mitsudomi, Y. Song, C. Hyland, J.O. Park, N. Lindeman, C.M. Gale, X. Zhao, J. Christensen, T. Kosaka, A.J. Holmes, A.M. Rogers, F. Cappuzzo, T. Mok, C. Lee, B.E. Johnson, L.C. Cantley, P.A. Janne, MET amplification leads to gefitinib resistance in lung cancer by activating ERBB3 signaling, Science 316 (2007) 1039–1043.
[19] D.L. Shattuck, J.K. Miller, K.L. Carraway 3rd, C. Sweeney, Met receptor contributes to trastuzumab resistance of Her2-overexpressing breast cancer cells, Cancer Res. 68 (2008) 1471–1477.
[20] P.M. Comoglio, S. Giordano, L. Trusolino, Drug development of MET inhibitors: targeting oncogene addiction and expedience, Nat. Rev. Drug Discov. 7 (2008) 504–516.
[21] T.L. Underiner, T. Herbertz, S.J. Miknyoczki, Discovery of small molecule c-Met inhibitors: evolution and profiles of clinical candidates, Anticancer Agents Med. Chem. 10 (2010) 7–27.
[22] J.J. Cui, Inhibitors targeting hepatocyte growth factor receptor and their potential therapeutic applications, Expert Opin. Ther. Patents 17 (2007) 1035–1045.
[23] H.M. Berman, J. Westbrook, Z. Feng, G. Gilliland, T.N. Bhat, H. Weissig, I.N. Shindyalov, P.E. Bourne, The protein data bank, Nucleic Acids Res. 28 (2000) 235–242.
[24] R. Capdeville, E. Buchdunger, J. Zimmermann, A. Matter, Glivec (STI571, imatinib), a rationally developed, targeted anticancer drug, Nat. Rev. Drug Discov. 1 (2002) 493–502.
[25] T. Schindler, W. Bornmann, P. Pellicena, W.T. Miller, B. Clarkson, J. Kuriyan, Structural mechanism for STI-571 inhibition of abelson tyrosine kinase, Science 289 (2000) 1938–1942.
[26] Y. Liu, N.S. Gray, Rational design of inhibitors that bind to inactive kinase conformations, Nat. Chem. Biol. 2 (2006) 358–364.
[27] M.D. Jacobs, P.R. Caron, B.J. Hare, Classifying protein kinase structures guides use of ligand-selectivity profiles to predict inactive conformations: structure of lck/imatinib complex, Proteins 70 (2008) 1451–1460.
[28] Y. Asses, V. Leroux, S. Tairi-Kellou, R. Dono, F. Maina, B. Maigret, Analysis of c-Met kinase domain complexes: a new specific catalytic site receptor model for defining binding modes of ATP-competitive ligands, Chem. Biol. Drug Des 74 (2009) 560–570.
[29] I. Dussault, S.F. Bellon, c-Met inhibitors with different binding modes: two is better than one, Cell Cycle 7 (2008) 1157–1160.
[30] N. Schiering, S. Knapp, M. Marconi, M.M. Flocco, J. Cui, R. Perego, L. Rusconi, C. Cristiani, Crystal structure of the tyrosine kinase domain of the hepatocyte growth factor receptor c-Met and its complex with the microbial alkaloid K-252a, Proc. Natl. Acad. Sci. U S A 100 (2003) 12654–12659.
[31] S.F. Bellon, P. Kaplan-Lefko, Y. Yang, Y. Zhang, J. Moriguchi, K. Rex, C.W. Johnson, P.E. Rose, A.M. Long, A.B. O'Connor, Y. Gu, A. Coxon, T.S. Kim, A. Tasker, T.L. Burgess, I. Dussault, c-Met inhibitors with novel binding mode show activity against several hereditary papillary renal cell carcinoma-related mutations, J. Biol. Chem. 283 (2008) 2675–2683.
[32] S. Patane, N. Pietrancosta, H. Hassani, V. Leroux, B. Maigret, J.L. Kraus, R. Dono, F. Maina, A new Met inhibitory-scaffold identified by a focused forward chemical biological screen, Biochem. Biophys. Res. Commun. 375 (2008) 184–189.
[33] Z.W. Cai, D. Wei, G.M. Schroeder, L.A. Cornelius, K. Kim, X.T. Chen, R.J. Schmidt, D.K. Williams, J.S. Tokarski, Y. An, J.S. Sack, V. Manne, A. Kamath, Y. Zhang, P. Marathe, J.T. Hunt, L.J. Lombardo, J. Fargnoli, R.M. Borzilleri, Discovery of orally active pyrrolopyridine- and aminopyridine-based Met kinase inhibitors, Bioorg. Med. Chem. Lett. 18 (2008) 3224–3229.
[34] N.D. D'Angelo, S.F. Bellon, S.K. Booker, Y. Cheng, A. Coxon, C. Dominguez, I. Fellows, D. Hoffman, R. Hungate, P. Kaplan-Lefko, M.R. Lee, C. Li, L. Liu, E. Rainbeau, P.J. Reider, K. Rex, A. Siegmund, Y. Sun, A.S. Tasker, N. Xi, S. Xu, Y. Yang, Y. Zhang, T.L. Burgess, I. Dussault, T.S. Kim, Design, synthesis, and biological evaluation of potent c-Met inhibitors, J. Med. Chem. 51 (2008) 5766–5779.
[35] M. Amat, A. Kövér, D. Jokic, O. Lozano, M. Pérez, N. Landoni, F. Subrizi, J. Bautista, J. Bosch, Synthesis of a tetrahydroimidazo[2′,1′:2,3]thiazolo[5,4-c] pyridine derivative with Met inhibitory activity, ARKIVOC 3 (2010) 145–151.
[36] G.K. Chan, B.A. Lutterbach, B.S. Pan, I. Kariv, A.A. Szewczak, High-throughput analysis of HGF-stimulated cell scattering, J. Biomol. Screen. 13 (2008) 847–854.
[37] M. Sattler, Y.B. Pride, P. Ma, J.L. Gramlich, S.C. Chu, L.A. Quinnan, S. Shirazian, C. Liang, K. Podar, J.G. Christensen, R. Salgia, A novel small molecule met inhibitor induces apoptosis in cells transformed by the oncogenic TPR-MET tyrosine kinase, Cancer Res. 63 (2003) 5462–5469.
[38] H.Y. Zou, Q. Li, J.H. Lee, M.E. Arango, S.R. McDonnell, S. Yamazaki, T.B. Koudriakova, G. Alton, J.J. Cui, P.P. Kung, M.D. Nambu, G. Los, S.L. Bender, B. Mroczkowski, J.G. Christensen, An orally available small-molecule inhibitor of c-Met, PF-2341066, exhibits cytoreductive antitumor efficacy through anti-proliferative and antiangiogenic mechanisms, Cancer Res. 67 (2007) 4408–4417.
[39] K.M. Nicholson, C.H. Streuli, N.G. Anderson, Autocrine signalling through erbB receptors promotes constitutive activation of protein kinase B/Akt in breast cancer cell lines, Breast Cancer Res. Treat. 81 (2003) 117–128.
[40] S.Y. Wang, B. Chen, Y.Q. Zhan, W.X. Xu, C.Y. Li, R.F. Yang, H. Zheng, P.B. Yue, S.H. Larsen, H.B. Sun, X. Yang, SU5416 is a potent inhibitor of hepatocyte growth factor receptor (c-Met) and blocks HGF-induced invasiveness of human HepG2 hepatoma cells, J. Hepatol. 41 (2004) 267–273.
[41] F. Qian, S. Engst, K. Yamaguchi, P. Yu, K.A. Won, L. Mock, T. Lou, J. Tan, C. Li, D. Tam, J. Lougheed, F.M. Yakes, F. Bentzien, W. Xu, T. Zaks, R. Wooster, J. Greshock, A.H. Joly, Inhibition of tumor cell growth, invasion, and metastasis by EXEL-2880 (XL880, GSK1363089), a novel inhibitor of HGF and VEGF receptor tyrosine kinases, Cancer Res. 69 (2009) 8009–8016.
[42] N. Munshi, S. Jeay, Y. Li, C.R. Chen, D.S. France, M.A. Ashwell, J. Hill, M.M. Moussa, D.S. Leggett, C.J. Li, ARQ 197, a novel and selective inhibitor of the human c-Met receptor tyrosine kinase with antitumor activity, Mol. Cancer Ther. 9 (2010) 1544–1553.
[43] G. Jones, P. Willett, R.C. Glen, Molecular recognition of receptor sites using a genetic algorithm with a description of desolvation, J. Mol. Biol. 245 (1995) 43–53.
[44] G. Jones, P. Willett, R.C. Glen, A.R. Leach, R. Taylor, Development and validation of a genetic algorithm for flexible docking, J. Mol. Biol. 267 (1997) 727–748.
[45] M.L. Verdonk, J.C. Cole, M.J. Hartshorn, C.W. Murray, R.D. Taylor, Improved protein-ligand docking using GOLD, Proteins 52 (2003) 609–623.
[46] W.L. Jorgensen, D.S. Maxwell, J. Tirado-Rives, Development and testing of the OPLS all-atom force field on conformational energetics and properties of organic liquids, J. Am. Chem. Soc. 118 (1996) 11225–11236.
[47] N. Pietrancosta, F. Maina, R. Dono, A. Moumen, C. Garino, Y. Laras, S. Burlet, G. Quelever, J.L. Kraus, Novel cyclized Pifithrin-alpha p53 inactivators: synthesis and biological studies, Bioorg. Med. Chem. Lett. 15 (2005) 1561–1564.
[48] Q. Chao, K.G. Sprankle, R.M. Grotzfeld, A.G. Lai, T.A. Carter, A.M. Velasco, R.N. Gunawardane, M.D. Cramer, M.F. Gardner, J. James, P.P. Zarrinkar, H.K. Patel, S.S. Bhagwat, Identification of N-(5-tert-butyl-isoxazol-3-yl)-N′-{4-[7-(2-morpholin-4-yl-ethoxy)imidazo[2 ,1-b][1,3]benzothiazol-2-yl]phenyl}urea dihydrochloride (AC220), a uniquely potent, selective, and efficacious FMS-like tyrosine kinase-3 (FLT3) inhibitor, J. Med. Chem. 52 (2009) 7808–7816.
[49] J. Segarra, L. Balenci, T. Drenth, F. Maina, F. Lamballe, Combined signaling through ERK, PI3K/AKT, and RAC1/p38 is required for Met-triggered cortical neuron migration, J. Biol. Chem. 281 (2006) 4771–4778.
[50] F. Lamballe, M. Genestine, N. Caruso, V. Arce, S. Richelme, F. Helmbacher, F. Maina, Pool-specific regulation of motor neuron survival by neurotrophic support, J Neurosci. 31 (2011) 11144–11158.